FABRIZIO MARCELINO MINUTOLO

THE INFLUENCE OF DISSOLVED INORGANIC MACRONUTRIENT CONCENTRATION AND RATIO ON THE ELEMENTAL STOICHIOMETRY OF SINKING PARTICULATE MATTER AND CARBON EXPORT IN THE PERUVIAN UPWELLING SYSTEM

UNIVERSIDADE DO ALGARVE
Faculdade de Ciências e Tecnologia
2017

FABRIZIO MARCELINO MINUTOLO

THE INFLUENCE OF DISSOLVED INORGANIC MACRONUTRIENT CONCENTRATION AND RATIO ON THE ELEMENTAL STOICHIOMETRY OF SINKING PARTICULATE MATTER AND CARBON EXPORT IN THE PERUVIAN UPWELLING SYSTEM

Master thesis in Marine Biology

Thesis was done under the guidance of:

Prof. Dr. Ulf Riebesell, GEOMAR – Helmholtz Centre for Ocean Research Kiel

Prof. Dr. Ana Barbosa, Faculty of Sciences and Technology, Centre of Marine and Environmental Investigation, University of Algarve

Dr. Lennart Bach, GEOMAR – Helmholtz Centre for Ocean Research Kiel

UNIVERSIDADE DO ALGARVE
Faculdade de Ciências e Tecnologia
2017

DECLARATION OF AUTHORSHIP

THE INFLUENCE OF DISSOLVED INORGANIC MACRONUTRIENT CONCENTRATION AND RATIO ON THE ELEMENTAL STOICHIOMETRY OF SINKING PARTICULATE MATTER AND CARBON EXPORT IN THE PERUVIAN UPWELLING SYSTEM

I declare to be the author of this thesis which is original and inedited. The authors and articles consulted are properly cited in the text and are included in the references list.
Declaro ser o autor deste trabalho, que é original e inédito. Autores e trabalhos consultados estão devidamente citados no texto e constam da listagem de referências incluída.

_____

(Fabrizio Marcelino Minutolo)

GEOMAR – Helmholtz Centre for Ocean Research Kiel, in collaboration with Instituto del Mar del Perú (IMARPE), provided experimental equipment and lab facilities.

Acknowledgements

I would like to thank Ulf Riebesell for allowing me to be part of the KOSMOS Peru 2017 experiment and to write my master thesis in his working group. Many thanks also go to Ana Barbosa, Lennart Bach, Paul Stange and Tim Boxhammer for scientific input and helpful comments. Furthermore, thank you to Jana Meyer for helping in processing the sediment trap samples. I would also like to thank Elisabeth von der Esch, Claudia Sforna and Kai Schulz for providing data on nutrients, Chl *a* and CTD profiles. And of course, thank you to my family and the entire KOSMOS Peru 2017 team for all kinds of support!

Abstract

Peruvian coastal waters are influenced by strong coastal upwelling events and an intense oxygen minimum zone, where large amounts of fixed nitrogen can be lost. In order to investigate some of the effects this oxygen minimum zone may have on these coastal waters, this study aimed to evaluate the influence of dissolved inorganic macronutrient concentration and ratio on the elemental stoichiometry of sinking particulate matter and carbon export. At the beginning of February 2017, eight mesocosms were deployed in coastal waters near Lima, Peru. 4 mesocosms were enriched with an OMZ derived water mass with a dissolved inorganic N:P ratio of 0.11, while the other 4 were enriched with OMZ water of N:P = 1.71. The amount of utilized reactive nitrogen was not associated to differences in carbon export rates, but the results of one individual mesocosm hint at stronger carbon export at low primary production. Furthermore, sinking particulate matter and its elemental stoichiometry did not show differences between treatments. However, our results showed clear deviations from the canonical Redfield ratio in sinking POM, hypothesized to be related with phytoplankton community composition.

Keywords: oxygen minimum zone, upwelling, nutrient ratio, POM elemental stoichiometry, vertical flux, carbon export

Resumo

Os nutrientes inorgânicos dissolvidos são fundamentais para o funcionamento das redes alimentares marinhas e são, direta ou indiretamente, absorvidos por todos os organismos vivos. As regiões de afloramento costeiro apresentam elevada concentração de nutrientes inorgânicos, constituindo ecossistemas marinhos muito produtivos a nível biológico. Embora representam apenas 1% da área superficial do oceano global, as áreas de afloramento costeiro são responsáveis, em média,por cerca de 11% da produção primária anual nova. A variabilidade climática prevista, associada à crescente da pressão antrópica na atmosfera e no oceano, foi associada à intensificação e expansão da área ocupada pelas zonas mínimas de oxigénio (*Oxygen Minimum Zones*, OMZ), geralmente associadas aos sistemas de afloramento costeiro. Neste contexto, torna-se necessário avaliar e compreender as consequências do aumento das OMZ sobre os ciclos biogeoquímicos de nutrientes, de forma a prever com rigor a variabilidade futura do ambiente marinho e aplicar estratégias de gestão adequadas.

Os eventos de afloramento costeiro ao largo da costa do Peru, bem como em outros sistemas similares, estão geralmente associados ao transporte de massas de água sub-superficiais, com elevada concentrações de nutrientes inorgânicos dissolvidos. Porém, a concentração de nutrientes inorgânicos dissolvidos e as proporções entre as formas contendo azoto e fósforo (*ratio* N:P) variam em função da intensidade dos eventos de afloramento e dos processos que influenciam a concentração e composição dos nutrientes em níveis inferiores à superfície. O azoto inorgânico é um elemento essencial ao crescimento do fitoplâncton e, muitas vezes, limita a produtividade primária, desempenhando assim um papel crucial na biogeoquímica marinha. As formas de azoto

inorgânico biodisponíveis incluem o nitrato, nitrito e amónia, mas constituem apenas cerca de 6% da concentração total de azoto disponível na água do mar.

O fósforo inorgânico é igualmente um elemento essencial ao crescimento do fitoplâncton, sendo a principal forma biodisponível o fosfato. Representa uma parte integrante da estrutura celular (ex.: ácidos nucleicos, incluindo DNA e RNA) e dos compostos associados ao armazenamento de energia química nas células, nomeadamente da molécula adenosina trifosfato (ATP). Assim, a análise do ciclo biogeoquimico do fósforo é relevante para determinar a estrutura e função dos ecossistemas.

A exportação vertical de matéria orgânica a partir da superfície do oceano representa um processo chave para o funcionamento da bomba biológica de carbono, um componente importante do ciclo global do carbono. O carbono inorgânico é absorvido sob a forma de CO_2 pelo fitoplâncton, transformado e acumulado no interior das células sob a forma de carbono orgânico, através da fotossíntese, e transportado verticalmente para o oceano profundo. Assim, o fluxo vertical de células fitoplanctónicas, em estado fisiológico variável, controla fortemente a capacidade do oceano como um coletor e reservatório de CO_2. A exportação vertical de material particulado é determinada pela taxa de decomposição e velocidade de afundamento do material em afundamento, bem como pela migração vertical diária do zooplâncton ativo. O material particulado em afundamento no oceano é composto por agregados orgânicos, geralmente designados neve marinha, pelotas fecais do zooplâncton e fitodetritos. As partículas com reduzida velocidade de afundamento são geralmente consumidas ou degradadas antes de atingir o oceano profundo. Pelo contrário, as partículas com elevada velocidade de afundamento apresentam maior probabilidade de atingir o sedimento. A eficiência da bomba biológica depende ainda da composição da

comunidade fitoplanctónica e, em consequência, das condições abióticas do ambiente marinho, incluindo a concentração e composição dos nutrientes inorgânicos dissolvidos.

O presente estudo pretende avaliar a influência da concentração e composição (ratio) dos macronutrientes inorgânicos dissolvidos na água aflorada sobre a estequiometria da matéria em suspensão na plataforma continental do Peru. Os objetivos específicos do estudo abordaram as seguintes questões: (1) Estarão massas de água afloradas com diferente concentração e composição de nutrientes (ratio N:P) associadas a diferenças na estequiometria elementar das partículas em suspensão e sedimentação?; (2) Estarão a concentração e a taxa de absorção de nutrientes relacionadas com diferenças nas taxas de exportação do carbono orgânico?

O presente estudo integrou-se no Collaborative Research Center (SFB 754) "Climate-Biogeochemistry Interactions in the Tropical Ocean" e baseou-se numa experiência iniciada em fevereiro de 2017, com recurso à plataforma Kiel Off-Shore Mesocosms for Ocean Simulations (KOSMOS), uma instalação móvel de mesocosmos, aplicável em experiências em larga escala, in situ. Os mesocosmos são unidades experimentais com um volume elevado, apropriadas para simular eventos de afloramento, em condições controladas *quasi* naturais, uma vez que permitem a manipulação eficiente das variáveis ambientais, incluindo a concentração de nutrientes. De forma a atingir os objetivos propostos, foram utilizados dois tratamentos experimentais, com quatro replicados cada (2 * 4 = 8 mesocosmos): massa de água com ratio N:P reduzido e massa de água com ratio N:P muito reduzido, a nível da composição de nutrientes inorgânicos dissolvidos. No início de fevereiro de 2017, foram implantados oito mesocosmos em águas costeiras ao largo de Lima (Peru), contendo armadilhas de sedimento no interior. A experiência decorreu durante um período de 50 dias, entre fevereiro e abril de 2017. Quatro mesocosmos foram enriquecidos com uma

massa de água amostrada na OMZ, com um ratio N: P de 0,11, enquanto os restantes quatro mesocosmos foram enriquecidos com uma massa de água amostrada na OMZ com um ratio N: P de 1,71. Em cada um dos oito mesocosmos foram analisadas a concentração de nitritos, nitratos, amónia, fosfatos, silicatos, bem como os ratio associados, e clorofila-a (indicador da biomassa total do fitoplâncton) na coluna de água. Adicionalmente, foi amostrada a matéria particulada acumulada no interior de armadilhas de sedimento. Neste caso foram analisadas a concentração de carbono total, azoto total, carbono orgânico particulado, azoto orgânico particulado, carbono inorgânico particulado, sílica orgânica particulada e sílica biogênica. As diferenças entre os dois tratamentos experimentais, para todas as variáveis referidas, foram testadas estatisticamente.

Os resultados obtidos não revelaram diferenças significativas em nenhuma das variáveis químicas ou biológicas entre os dois tratamentos experimentais. No entanto, observaram-se desvios claros nos ratios C: N: P, em relação aos valores propostos por Redfield (106: 16: 1), para os nutrientes inorgânicos dissolvidos e matéria orgânica particulada acumulada nas armadilhas de sedimento. Hipóteses para explicar estes desvios foram apresentadas, incluindo variações na composição da comunidade de fitoplâncton e mixotrofia. Os resultados indicaram que a concentração de azoto utilizado não se associou a diferenças significativas nas taxas de exportação vertical de carbono. No geral, a estratégia experimental utilizada apresentou alguns problemas incluindo uma similaridade entre as duas massas de água amostradas na OMZ e os distúrbios gerados pelas aves marinhas (ex.: entrada de guano e presas no interior dos mesocosmos). Experiências futuras deverão ativamente limitar estes problemas. A informação quantitativa sobre a composição da comunidade fitoplanctónica, disponível futuramente (após a data de submissão desta tese de mestrado), deverá ser utilizada para testar as hipóteses apresentadas no estudo.

Table of content

Index of abbreviations

BSi	biogenic silica
°C	degree Celsius
Chl	chlorophyll
cm	centimetre
cum	cumulative
DIC	dissolved inorganic carbon
DOC	dissolved organic carbon
DON	dissolved organic nitrogen
g	gram
h	hour
L	litre
min	minute
N	nitrogen
µg	micro gram
µmol	micro mol
P	phosphorous
PAR	photosynthetically active radiation
PIC	particulate inorganic carbon
POC	particulate organic carbon
POM	particulate organic matter
PON	particulate organic nitrogen
POP	particulate organic phosphorus
PP	primary production
SED	sediment trap
SST	sea surface temperature
TPC	total particulate carbon
TPN	total particulate nitrogen

1. Introduction

1.1 Coastal upwelling ecosystems and Oxygen Minimum Zones

The eastern boundaries of the Atlantic and Pacific Oceans are characterized by major coastal upwelling systems. Prevailing alongshore equatorward wind stress, in combination with Coriolis deflection due to earth´s rotation, forces surface water to be driven offshore, which in turn is replaced by cool, nutrient-rich subsurface upwelled water (Bakun, 1990; Caddy and Bakun, 1994). These coastal upwelling areas therefore supply essential dissolved inorganic nutrients and stimulate phytoplankton primary production, which forms the base of productive food webs, including valuable fishery resources (Bakun, 1990). Coastal upwelling regions cover only a small fraction (1%) of the global ocean, but contribute disproportionally to oceanic productivity, therefore playing an important role in the biogeochemical cycling of marine nutrients (Capone and Hutchins, 2013; Hauss, Franz and Sommer, 2012). The Peru current system, flowing northwards off the South American West coast, is unequaled among all other upwelling systems in terms of fish biomass and fishery landings (Bakun and Weeks, 2008). Biogeochemically, it is also of great importance due to its intense Oxygen Minimum Zone (OMZ), with a thickness over 600m at some points (Daneri et al., 2000; Fuenzalida et al., 2009). OMZs are permanently oxygen deficient waters that develop at mid-depths, below surface waters, as a result of poor ventilation, high surface primary production and resultant organic matter vertical exportation which is decomposed by microbial activity, ultimately consuming oxygen (Fuenzalida et al., 2009; Kalvelage et al., 2013). As anthropogenic disturbances continue to support global warming and oceanic nutrient input, further decreasing oxygen concentrations in the ocean, OMZs are predicted to increase both in spatial coverage and intensity (Fuenzalida et al., 2009).

Even though OMZs with oxygen concentrations less than 20 µmol kg^{-1} occupy only 1% of the global ocean volume, they account for ~20-40% of global oceanic nitrogen loss (Glock et al., 2013; Lam and Kuypers, 2011).

1.2 Nitrogen cycling in Oxygen Minimum Zones

Inorganic nitrogen is essential for phytoplankton growth and often limits marine primary productivity, therefore playing a crucial role within marine biogeochemistry (Bohlen et al., 2011; Glock et al., 2013). Bioavailable forms of inorganic nitrogen include nitrate (NO_3^-), nitrite (NO_2^-) and ammonium (NH_4^+), but constitute only 6% of total nitrogen available in seawater (Bohlen et al., 2011; Gier et al., 2016). A generalization of the marine nitrogen cycle is depicted in Figure 1.1.

Under oxic conditions (>90 µmol O_2 kg^{-1}), present in most parts of the global ocean, oxygen is the most energetically favourable electron acceptor for the decomposition of organic matter (Lam and Kuypers, 2011; Kristensen, 2000). However, in oxygen depleted waters, nitrate is the next preferred electron acceptor and used as an oxidant in the degradation of sinking organic matter, yielding similar amounts of free energy in relation to oxic microbial respiration (Lachkar et al., 2016; Lam and Kuypers, 2011). This dissimilatory reduction of nitrate in anaerobic respiration converts nitrate, with intermediate products, to dinitrogen gas (N_2), thus resulting in a lower N:P nutrient ratio and therefore a deficit of nitrate relative to phosphate (Fuenzalida et al., 2009). Increasing denitrification rates, the complete reduction of nitrate to N_2, due to decreasing oxygen concentrations, lead to a lower nitrogen inventory in the ocean, thus negatively affecting marine productivity. Moreover, denitrification is positively linked to nitrous oxide (N_2O) production and release to the

atmosphere. This in turn will result in higher atmospheric CO_2 and nitrous oxide (N_2O) levels, further supporting the greenhouse effect (Gruber, 2008).

Anaerobic ammonium oxidation (anammox), based on NO_2^- as final electron accepter, is another biological process associated to N_2 gas production. Anammox is carried out by chemo-autotrophic bacteria, meaning that the reaction is used as an energy source. In contrast to denitrification, anammox is associated to the emission of N_2 without the production of intermediate, powerful greenhouse gases (e.g., N_2O). More and more attention is being attributed to this relatively recently discovered process in the marine environment, as its quantitative significance for the marine nitrogen cycle is not fully known yet (Brandes et al., 2007; Gruber, 2008). At least one study (Kuypers et al., 2005) has suggested that anammox, instead of denitrification, is primarily responsible for the biological loss of fixed nitrogen in the OMZ of the Benguela upwelling system. However, it is important to keep in mind that processes supplying the reactants for annamox (or other reactions in general) may differ in intensity across different environments. Therefore, the contribution of anammox to the loss of fixed nitrogen in the Peru upwelling system might be very variable (Brandes et al., 2007; Gruber, 2008).

Heterotrophic denitrification and anammox are the two dominant pathways through which atmospheric N_2 is released and reactive nitrogen is lost, thus lowering the inorganic N:P stoichiometry (Franz et al., 2012b; Glock et al., 2013). Nitrate reduction and dissimilatory nitrate reduction to ammonium (DNRA), another nitrate consuming process occurring under suboxic and anoxic conditions, have been identified in the Peruvian OMZ, and suggested to sometimes provide most of the NO_2^- and NH_4^+ needed for anammox, respectively (Glock et al., 2013; Lam et al., 2009). Both heterotrophic and chemolithoautotrophic organisms are

able to carry out DNRA (Giblin et al., 2013). DNRA, unlike denitrification and anammox, conserves reactive N within the ecosystem as ammonium, which may be incorporated by organisms or oxidized back to nitrate. Most studies on DNRA have been carried out in sulfide-rich environments, with some of them showing that DNRA can be a major pathway for nitrogen (Giblin et al., 2013; Glock et al., 2013; Lam et al., 2009).

Atmospheric N_2 is converted to organic nitrogen by nitrogen fixing bacteria, which are the only organisms in the marine realm that can access the large pool of dinitrogen gas (Bohlen et al., 2011; Glock et al., 2013). Marine N_2 fixation is mainly associated to photoautotrophic cyanobacteria (e.g. diazotrophs), and is the most important source of fixed new nitrogen when nitrogen concentrations are exhausted (Gruber, 2008). Fixed organic nitrogen is mostly remineralized to nitrate by two consecutive processes: ammonification and nitrification. Firstly, organic nitrogen is converted to NH_4^+ (ammonification) by heterotrophic bacteria, mostly. Then nitrifying prokaryotes carry out nitrification, by facilitating the oxidation of NH_4^+ to NO_2^- and the oxidation of NO_2^- to NO_3^-. It must be noted that nitrification is an aerobic process. Therefore, the expected expansion of OMZs could inhibit global nitrification rates (Glock et al., 2013; Gruber, 2008).

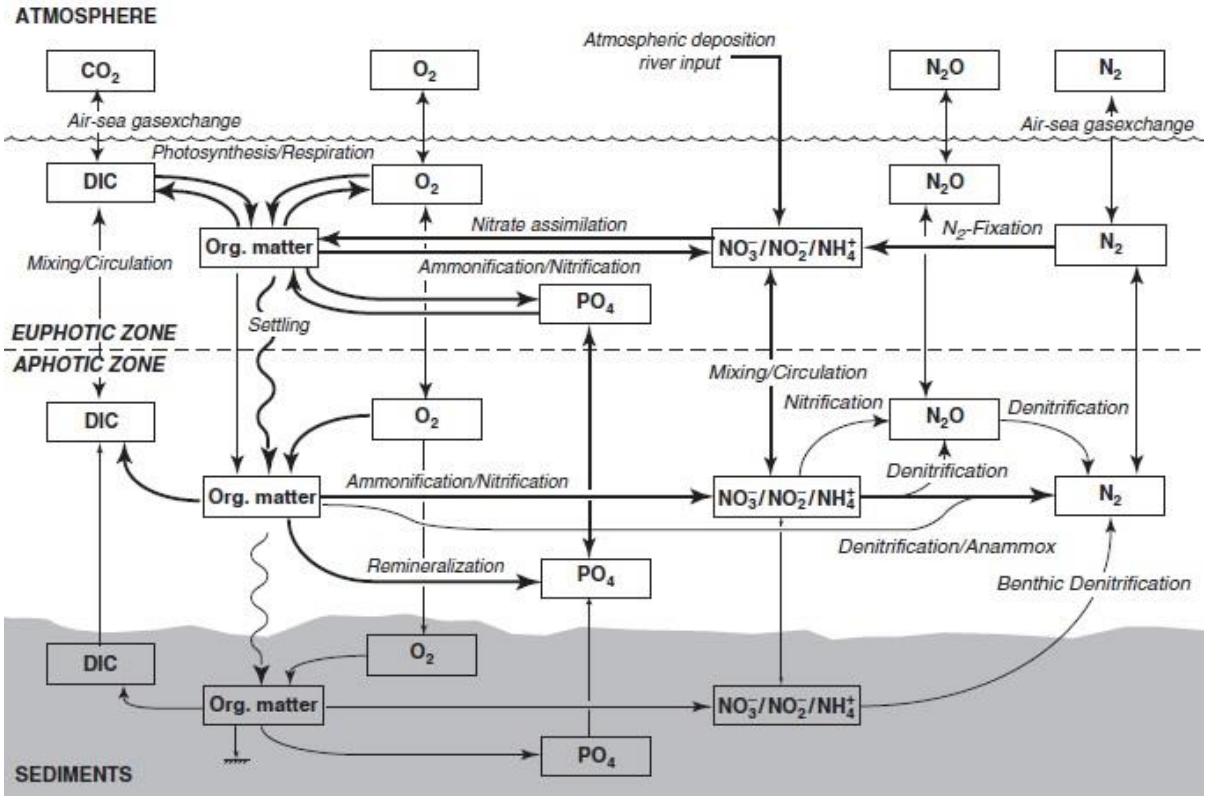

Figure 1.1: Schematic representation of the marine nitrogen cycle and its coupling to the marine cycles of oxygen, phosphorous and carbon. Of particular importance are the processes of nitrogen fixation and denitrification, which make the fixed nitrogen content of the ocean open to biologically mediated changes. Note that dissimilatory nitrate reduction to ammonium (DNRA) is not included. Extracted from Gruber (2008).

1.3 Phosphorous cycling in Oxygen Minimum Zones

Another essential inorganic nutrient for phytoplankton growth and life in general is phosphorus (P), being an integral part for energy storage and cell structure (Filippelli, 2001; Elser et al., 2007; White and Dyhrman, 2013). P is an essential part of adenosine triphosphate (ATP), therefore playing a major role in the transmission of chemical energy. Additionally, P is crucial for the structural framework of nucleic acids, including DNA and RNA (Paytan and McLaughlin, 2007). Thus, in order to determine ecosystem structure and function, the biogeochemical cycling of phosphorus is important and must be addressed (White and Dyhrman, 2013). An overview of the marine phosphorous cycle is illustrated in Figure 1.2. Unlike N, there are no organisms that can fix P from the atmosphere. Therefore,

P is often the limiting macronutrient for primary production over geological time scales (Paytan and McLaughlin, 2007). Like N, P partly governs the velocity at which atmospheric CO_2 is taken up and converted to organic matter, therefore influencing the marine carbon cycle (Föllmi, 1996; Paytan and McLaughlin, 2007). Distribution patterns and processes of dissolved inorganic phosphorus (DIP) have been studied more intensively than those of dissolved organic phosphorus (DOP). However, relatively recent studies revealed the importance of DOP as a phosphorus source for marine primary producers. In surface waters of coastal marine systems, DOP represents a major part of dissolved phosphorus and can comprise up to ~90% of total dissolved phosphorus (TDP) (Ruttenberg and Dyhrman, 2012; White and Dyhrman, 2013). DOP is converted to bioavailable DIP through the enzymatic hydrolysis of organic substrates, by alkaline phosphatase and C-P lyase (Ruttenberg and Dyhrman, 2012). Ruttenberg and Dyhrman (2012) showed how changes in inorganic N:P ratios affect DOP production in coastal upwelling areas, by taking advantage of the fact that low concentrations of DIP induce the activity of alkaline phosphatase, thereby increasing the DIP concentration by converting DOP to DIP.

The dominant input of phosphorus to the oceans is associated to continental weathering. Much of this input is retained within continental shelve sediments, as particulate phosphorus (Froelich et al., 1982; Paytan and McLaughlin, 2007). Within sediments, P is present as organic and inorganic forms. The fraction of organic P is very small compared to the bulk sediment weight, and usually is much less concentrated than DIP. Inorganic forms are iron and –calcium-bound and exhibit particular sensitivity to variations in the redox potential. Iron-bound P usually occurs in oxic surface sediments, while anoxic sediments are more abundant in calcium-bound P (Gomez et al., 1999; Paytan and McLaughlin, 2007).

After burial, iron dissolution, phosphate release and the precipitation of apatite (phosphorus rich mineral) may occur through various biotic and abiotic processes (White and Dyhrman, 2013). Generally, phosphorite deposits are interpreted as proxies for periods and/or locations of high biological production, as well as low oxygen concentration at the sediment-water interface, not only for geological records but also for modern day deposits. These phosphorite deposits have been identified at the continental margins of some of the major upwelling areas, including the Peru upwelling system (Paytan and McLaughlin, 2007).

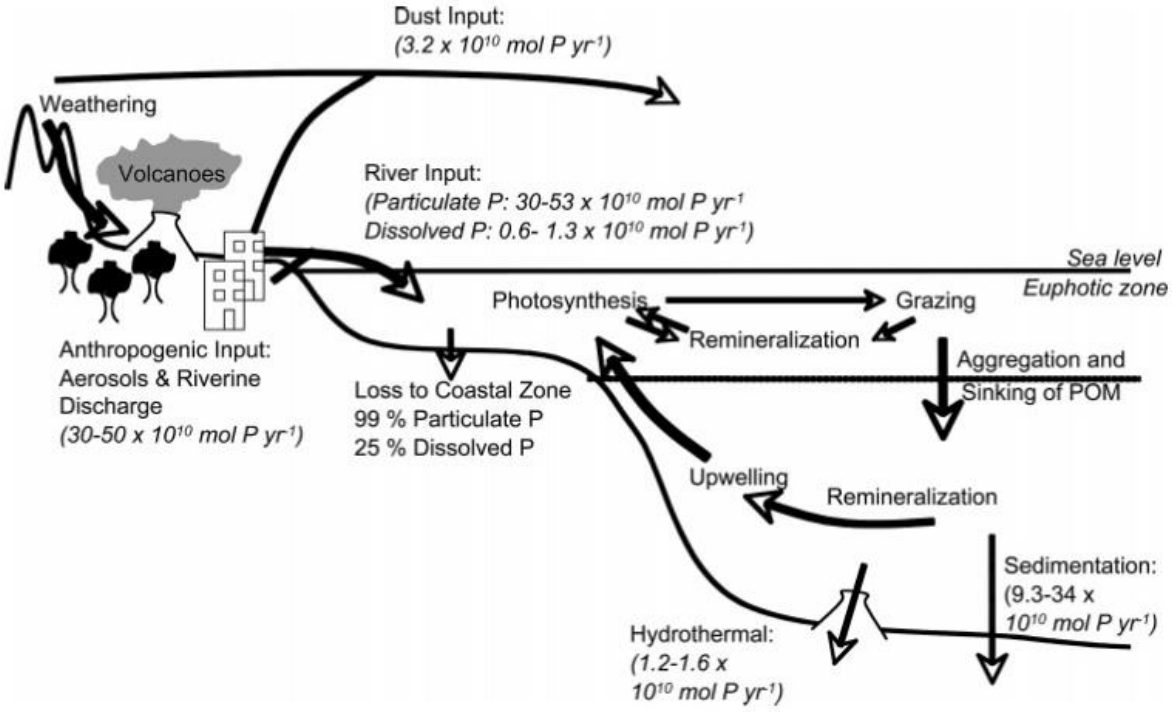

Figure 1.2: Schematic representation of the marine phosphorus cycle. Fluxes are given in italics. Continental weathering is the primary source of phosphorous to the oceanic phosphorous cycle. Most of this phosphorous is delivered via rivers, with a smaller portion delivered via dust deposition. In recent times, anthropogenic sources of phosphorous have become a large fraction of the phosphorous delivered to the marine environment, effectively doubling the pre-anthropogenic flux. The primary sink for phosphorous in the marine environment is loss to the sediments. Much of the particulate flux from rivers is lost to sediments on the continental shelves, and a smaller portion is lost to deep-sea sediments. Extracted from Paytan and McLaughlin (2007).

1.4 Importance of vertical flux and inorganic N:P

The vertical export of organic material from the surface of the ocean is a key process for the biological carbon pump, which is an important component of the global carbon cycle.

Carbon, taken up as CO_2 and accumulated in phytoplankton cells via photosynthesis, is transported to the deep ocean (Le Moigne et al., 2015; Riebesell et al., 2007). Thus, the vertical flux of phytoplankton cells is to some extent responsible for the ocean´s ability to act as a sink for CO_2 (Agusti et al., 2015). The vertical export of particulate matter is determined by the decomposition rate and sinking velocity of the sinking material, as well as active zooplankton vertical migration (Arístegui et al., 2009; Neuer, 2014). Sinking POM is composed of marine snow (i.e. organic aggregates), zooplankton fecal pellets and phytodetritus (Turner, 2015). Slow sinking particles are eaten or degraded before reaching greater depths, as opposed to faster sinking particles, which are likelier to reach the sediment (Neuer, 2014).

Nutrient and light availability modulate phytoplankton primary production and community composition. Therefore, it is necessary to establish a link between phytoplankton community composition and export efficiency, in order to understand how changing environments may influence the biological carbon pump (Le Moigne et al., 2015).

Recently, it has been recognized that the elemental stoichiometry of POM might deviate from the canonical Redfield ratio (Martiny et al., 2014). The composition of C:N:P of POM is dependent on phytoplankton community composition and physiological state. Therefore, observed values and trends of the elemental stoichiometry of sinking POM may be linked, at least in part, to phytoplankton assemblages (Quigg et al., 2003). However, it is important to keep in mind that during sinking, POM may be subjected to processes that alter C:N:P ratios (eg. remineralisation) (Deutsch and Weber, 2012; Le Moigne et al., 2015?).

These variations in elemental composition of particulate matter may be the result of different mechanisms (Martiny et al., 2013b). One such mechanism refers to a decreased

allocation of N in phytoplankton cells as cells become N-limited, commonly resulting in a higher cellular C:N ratio. Another mechanism, whereby elemental ratios of particulate matter are influenced, is autotrophic and heterotrophic organisms specifically removing elements from phytodetritus. Additionally, phytoplankton growing under light limiting conditions may accumulate less carbon storage polymers, linking this mechanism to a reduced cellular C:N ratio. Furthermore, another mechanism suggests that different phytoplankton taxa have unique elemental stoichiometries. The last mechanism refers to the specific growth rate strategy (Martiny et al., 2013b). Phytoplankton cells larger than 20 µm (microplankton) mainly rely on upwelled nitrate as a nitrogen source, while smaller cells (pico- and nanoplankton, 0.2 – 20 µm) are able to use regenerated nutrients (e.g., ammonium), even under limiting nutrient conditions. Moreover, the inorganic N:P ratio requirements of phytoplankton also vary across phytoplankton functional ecotypes, and may deviate from the canonical Redfield N:P ratio of 16:1 (Franz et al., 2012b; Hauss et al., 2012; Meyer et al., 2016; Redfield, 1958). This behaviour has been suggested to originate in the specific growth rate strategy of primary producers, which allows for the broad division of phytoplankton into two groups, the 'bloomers' and the 'survivalists'. 'Bloomers' predominantly are large-celled phytoplankton (e.g. diatoms and dinoflagellates). Their cellular entities contain low N:P ratio RNA. On the other hand, 'survivalists', mainly small-celled phytoplankton (pico- and nanoplankton), are characterized by a higher cellular N:P ratio (relative to 'bloomers'), synthesizing vast amounts of N:P rich proteins(Franz et al., 2012b).

The previously mentioned processes and the resulting changes in nutrient stoichiometry may lead to variations in the supply of dissolved nutrients to surface waters during

upwelling events. Therefore, dissolved inorganic macronutrient composition may affect phytoplankton communities, which in turn may influence the elemental stoichiometry of sinking POM (Gervais and Riebesell, 2001; Hauss et al., 2012; Meyer et al., 2016; Sommer et al., 2004).

This study aimed to evaluate the influence of the composition of dissolved inorganic macronutrients in upwelled water on the elemental stoichiometry of sinking particulate matter off the Peruvian continental shelf.

The specific objectives addressed the following questions:

(1) Are upwelled waters with different dissolved inorganic N:P ratios associated to differences in the elemental stoichiometry of sinking particulate matter?
(2) Are nutrient concentration and uptake related to differences in organic carbon export rates?

This study presents data from a large scale *in situ* mesocosm experiment, conducted in Peruvian coastal water from the end of February to the middle of April 2017. Two experimental treatments with different dissolved inorganic N:P ratio were established. In the eight mesocosms (four replicates per treatment) nitrite, nitrate, ammonium, phosphate and silicate, Chl *a* and dissolved inorganic N:P ratio in the water column, as well as total particulate carbon and nitrogen, particulate organic carbon and nitrogen, particulate inorganic carbon, particulate organic phosphorous and biogenic silica in the sediment traps was assessed and checked for differences between the two experimental treatments.

2. Materials and Methods

2.1 Study area

The Peruvian upwelling region is part of the eastern boundary current of the Eastern Tropical South Pacific (Bohlen et al., 2011). Despite the seasonal and interannual variations in upwelling intensity, this region is considered as one of the most productive marine ecosystems. The distribution of sea surface temperatures (SST) over the region, with a clear cross-shore gradient and colder temperatures onshore, represents the signature of coastal upwelling activity (Fig. 2.1A). Upwelled colder nutrient-rich water masses, with high concentrations of nitrate, phosphorus and silicate (Capone and Hutchins, 2013), lead to high levels of phytoplankton primary productivity, as indicated by high surface chlorophyll *a* concentration over the continental shelf (Fig. 2.1B). The high primary production at the surface and the consequent sinking of organic matter accompanied by oxic microbial respiration, gives rise to the most intense marine oxygen minimum zone (Gier et al., 2016).

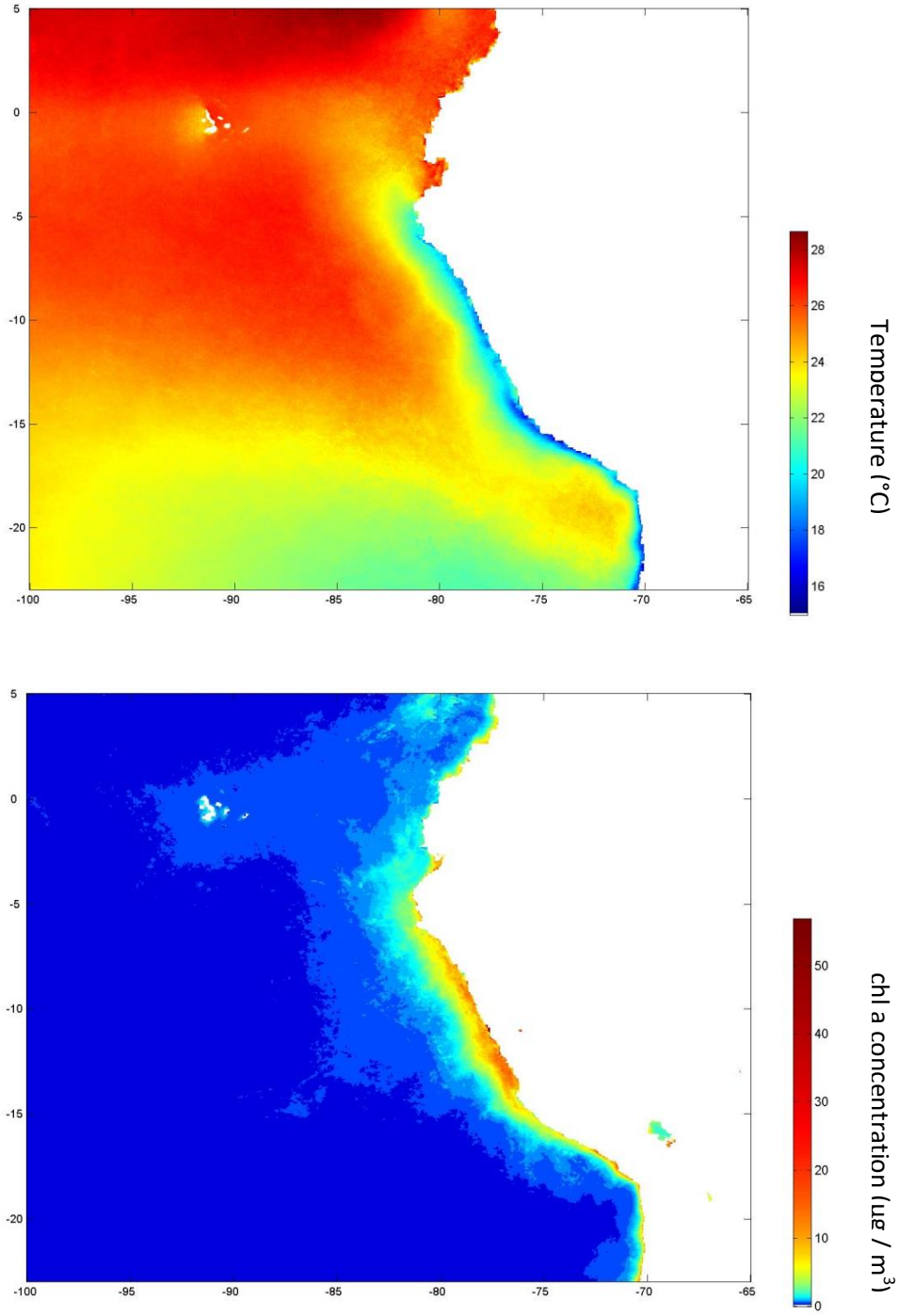

Figure 2.1: Mean distribution of (A) sea surface temperature and (B) surface Chl *a* concentration for the Peruvian upwelling region (between 5°N, 23°S, 100°W,65°W), at a 4km spatial resolution, during the period January-April 2010-2014 (approximate experimental period). Data were acquired from the MODerate-resolution Imaging Spectroradiometer satellite sensor (MODIS-Aqua) at https://oceancolor.gsfc.nasa.gov NASA. Analyses and visualizations were produced with the grid viewing program Mirone (Luis, 2007).

2.2 Experimental design

The influence of dissolved inorganic macronutrient ratios (i.e. N:P) on the elemental stoichiometry of sinking particulate matter and vertical exportation off the Peruvian continental shelf was investigated using a dedicated large scale *in situ* mesocosm experiment. The experiment was conducted from February to April 2017 and the mesocosm mooring site was located north of Isla San Lorenzo, off the Lima coast (12° 03.328' S, 077° 14.086' W; Fig. 2.2), within the region of maximum primary productivity of the Peruvian upwelling system (Bohlen et al., 2011; Bruland et al., 2005).

Figure 2.2: Mesocosm mooring site (red circle). Maps were acquired from the Bathymetry Data Viewer at https://maps.ngdc.noaa.gov/

2.2.1 Experimental units: Mesocosms

The *in situ* mesocosm experiment was based on the mobile sea-going Kiel Off-Shore Mesocosms for Ocean Simulations (KOSMOS) (Fig. 2.3A). This system includes eight mesocosm units. Each unit consists of a 20m long flexible polyurethane foil bag (2m in

diameter, 1mm thick; approximate capacity of 60 m^3), mounted to a metal flotation frame. At the bottom, each mesocosm unit is equipped with a sediment trap. The collection cylinder is connected to a sediment trap funnel to the top. To the bottom, it is connected to a silicon tube, which is attached to the flotation frame above the sea surface. A wire helix hose covers the first 1.5m of the silicon tube, to prevent current related bending of the tube (see details in Figure 2.3B). During deployment of the mesocosm units, the bags were sealed at the bottom and top with a 3mm mesh size net, to exclude large zooplankton and nekton from the experiment. Once lowered in the water column, the mesocosm bags were left open for approximately 3 days in order to ensure a complete exchange of the water body, thus promoting similar starting conditions inside all mesocosm units.

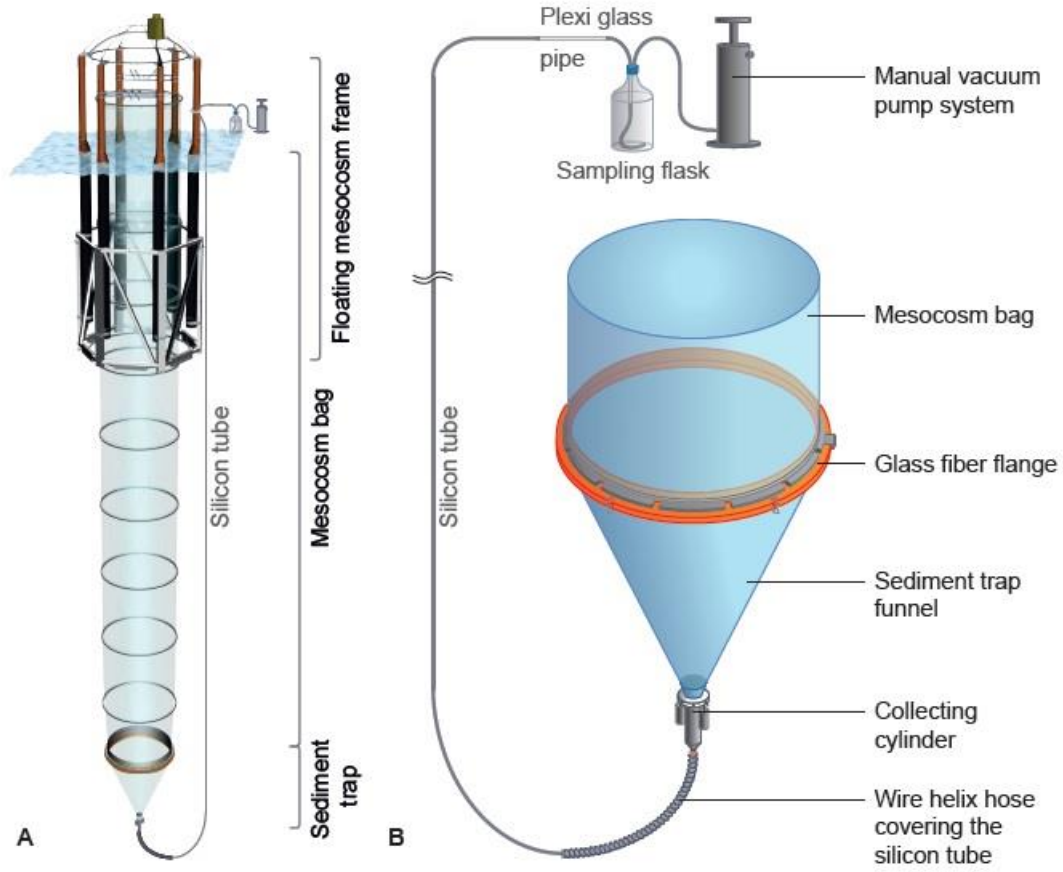

Figure 2.3: (**A)** Technical drawing of the Kiel Off-Shore Mesocosms for Ocean Simulations floating frame with the unfolded thermoplastic polyurethane enclosure bag and attached funnel-shaped sediment trap.(**B)**Sediment trap design and pumping system. Extracted from Boxhammer et al. (2015).

2.2.2 Evaluation of mesocosm volumes

The volume of each mesocosm was determined by using a dispersion device “spider” (Riebesell et al 2013), in order to evenly distribute a known amount of salt brine (52000g) to each of the mesocosm units. This was done via a pulley construction (Fig. 2.4) by gradually moving the spider up and down the entire mesocosm water column, while the salt brine (solution) was pumped through the “spider”. Salinity measurements were done before and after salt brine addition, using a multisensory CTD CTD60M (Sun and Sea Technologies). The resulting change in salinity, allowed the precise evaluation of mesocosm volume (see Czerny et al. 2013, for a detailed description).

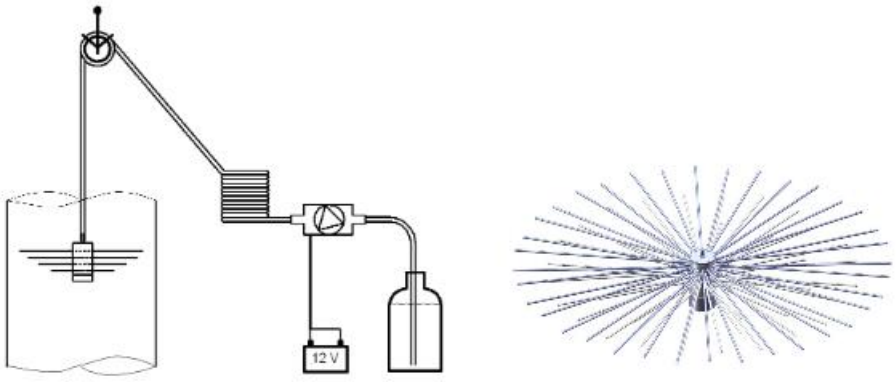

Fig 2.4: Sketch of the pulley construction used to move “spider” up and down (left). Dispersion device “spider” (right). Extracted from Riebesell et al., 2013

2.2.3 Experimental treatments

Two experimental treatments, with 4 replicates each, were prepared to test the effects of N:P nutrient ratios. OMZ influenced water masses, below the surface of the tropical South East Pacific, may have a remarkably low N:P ratio (relative to the Redfield ratio). Upwelling on the narrow continental shelf supplies surface waters with these water masses of low N:P ratio. N:P ratios below the Redfield ratio of 16:1 off the Peruvian coast have been identified,

and decreasing N:P ratios may be related to the expansion of OMZs (Franz et al., 2012a; Franz et al., 2012b).

OMZ water was collected at two different stations from a depth of approximately 40m, close to the seafloor, in the vicinity of the mooring site. After the deployment and closure of the eight mesocosms, known volumes (22000 L) of each of the two different OMZ derived water masses were added to the 4 replicate mesocosms of each experimental treatment, in order to stimulate upwelling. Prior to water addition, a slightly lower volume of water was pumped out of the mesocosms. For each mesocosm, OMZ water was added at two depth levels, mesocosm surface (0.5-9.0m) and bottom levels (14-17m), on day 12 (after sampling) and 11, respectively. The properties of the retrieved OMZ water masses are listed in Tables 2 and 3. Mesocosms 1, 4, 5 and 8 were used for the very low N:P treatment, while mesocosms 2, 3, 6 and 7 were used for the low N:P treatment.

2.3 Mesocosm sampling procedure

2.3.1 Water column sampling

Water samples were regularly collected during the experiment, starting after mesocosm closure (closure marked day 0). Sampling was undertaken every 48 hours, with the exception of the periods between days 1-4 and 12-18 where sampling was undertaken every 24 hours, always after sediment sampling. An integrating water sampler (IWS, Hydrobios) was used for dissolved inorganic macronutrients (NO_3^-, NO_2^-, NH_4^+, PO_4^{3-} and $Si(OH)_4^-$). Samples were transferred to acid-cleaned (10% HCl) plastic bottles, filtered through cellulose acetate filters (nominal pore size: 0.45 µm, GF/F, Whatman) to reduce

contamination effects, and analysed on the day of sampling. Suspended particulate matter was also sampled using integrating water samplers. During sampling, samples were protected from direct sunlight and stored in 5L canisters inside cooling boxes. Subsampling from canisters was done after manual homogenization, to ensure no particulate matter was accumulated at the carboy bottom. Concentration of both dissolved inorganic macronutrients and suspended particulate matter represented depth-integrated values for each mesocosm, since the sampling system allowed constant sampling of the entire water column, with homogeneous sampling throughout the entire mesocosm depth.

2.3.2 Sediment trap sampling

Sampling of the material accumulated inside the sediment traps was conducted every 48 hours, always before water sampling to avoid dispersion of the sediment trap material into the water column. The deposited material was (vacuum) pumped through the silicon tube and collected into 5L Schott Duran® glass flasks (Fig. 2.3B). At first sign of particles, visually detected through the Plexiglas® pipe, pumping was interrupted and seawater collected into the glass flasks was discarded, if clear. The vacuum sampling method was then reapplied. This sampling procedure ensured a minimized disturbance of the enclosed water body as well as an easy and efficient recovery of sedimented material. To avoid warming and increased bacterial degradation of the organic matter, glass flasks were stored inside large boxes, filled with cooling elements, throughout the sediment sampling and laboratory processing periods.

2.4 Sample analysis

2.4.1 Dissolved inorganic macronutrients

The concentration of dissolved NO_3^-, NO_2^-, NH_4^+, PO_4^{3-}, $Si(OH)_4^-$, was analysed directly after IWS sampling, using a SEAL Analytical QuAAtro AutoAnalyzer, connected to JASCO Model FP-2020 Intelligent Fluorescence Detector and a SEAL Analytical XY2 autosampler. Measurement procedures followed methods described by Hydes et al. (2010). For a detailed description of the determination of nitrite and nitrate, ammounium, phosphate and silicate, see Morris and Riley (1963), Kérouel and Aminot (1997), Murphy and Riley (1962) and Mullin and Riley (1965), respectively.

2.4.2 Suspended particulate matter

Subsamples were taken from the canisters for the analyses of chlorophyll a concentration (Chl *a*) and filtered onto combusted glass fibre filters (nominal pore size: 0.7 µm, 25 mm diameter, Whatman), using a gentle vacuum (< 200 mbar). Fluorometric determination of Chl *a* was carried out, using the method developed by Welschmeyer (1994).

2.4.3 Particulate matter accumulated inside sediment traps

After sediment sample collection and transport to laboratory facilities, sample volumes were determined gravimetrically. Subsamples (<10% of bulk sample volume) for other variables were taken after sample homogenization, by gently shaking the glass flasks. In order to separate sediment particles from (bulk) seawater, first, precipitation of the sediment trap particles was achieved by adding 3M $FeCl_3$ and 3M NaOH simultaneously at a ratio of 0,12 µl : 0,39 µl per gram of sample weight. The ratio of $FeCl_3$ to NaOH was previously determined, by adding increasing amounts of $FeCl_3$ to samples of day 0, until

maximum precipitation with minimal $FeCl_3$ input was visually determined. NaOH was then added until the pH values of the samples were close to 8,1 again. After 1 hour of settling time, the clear supernatant was carefully removed, using a vacuum pump. The remaining particle suspensions inside the 5L sampling flasks were then transferred to 800mL centrifuge beakers, and centrifuged for ~10 min at 5236 xg using a 6-16 KS centrifuge (Sigma). To prevent particle re-suspension, a slow deceleration was applied. After carefully discarding the supernatant, the remaining sample pellets were transferred into 110mL centrifuge tubes and the same procedure was applied until the 5L sampling flasks are empty. The small tubes were then centrifuged for ~10 min at 5039 xg, using a 3K12 centrifuge (Sigma) and after discarding the supernatant, the sediment pellets were immediately frozen at -20°C, inside plastic screw cap cups. Freeze-drying the sediment pellet samples for up to 72 hours removed the remaining water. Once all the water has been removed, sample pellets were enclosed inside a hollow sphere of 4VA steel, deep-frozen in liquid nitrogen, and ground into a homogeneous fine powder using the ball-mill developed by Boxhammer et al. (2015). The steps involved from sediment sample collection to grinding are summarized in Figure 2.5. For more details see Boxhammer et al. (2015).

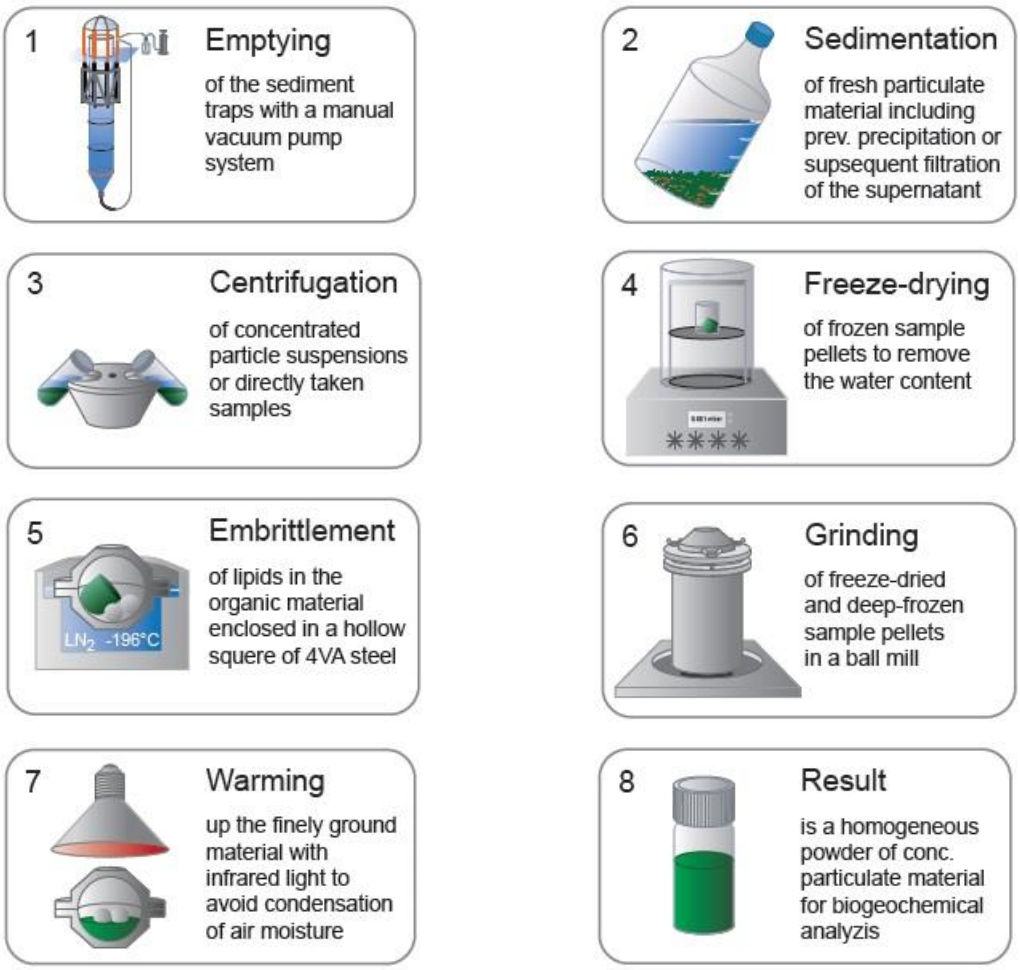

Figure 2.5: Protocol for mesocosm sediment trap sampling (1), particle concentration (2-3), freeze-drying (4) and grinding (5-8) to convert heterogeneous sediment trap samples into homogeneous powder for biogeochemical analysis. Adapted from Boxhammer et al. (2015).

Subsamples of the sediment pellet powder were used to determine the concentration of total particulate carbon (TPC_{SED}), nitrogen (TPN_{SED}), particulate organic phosphorous (POP_{SED}), biogenic silicate (BSi_{SED}), particulate organic carbon (POC_{SED}) and nitrogen (PON_{SED}). Two mg subsamples were transferred into tin cups and TPC_{SED}, TPN_{SED}, POC_{SED} and PON_{SED} was measured using an elemental analyser (Euro EA-CN, Hekatech), calibrated with acetanilide (C_8H_9NO) and soil standard (Hekatech, catalogue number HE33860101). PIC_{SED} was calculated by subtracting POC_{SED} from TPC_{SED}.

For POP_{SED} analysis, two mg subsamples were placed into 40 mL glass vials, containing a 40mL solution of deionized water and an oxidizing decomposition reagent (Merck, catalogue no. 112936). Particulate organic phosphorous was oxidized to orthophosphate by autoclaving at 121^{o}C for 30 minutes in a pressure cooker. After sample cooling, a spectrophotometric analysis, similar to the method of Hansen and Koroleff (1999) for dissolved inorganic phosphorous, was used to determine POP_{SED} concentrations.

BSi_{SED} from the sediment pellet powder was leached by alkaline pulping with 0.1 M NaOH at 85°C for 135 minutes. Adding 0.05 M H_2SO_4 terminated the leaching process, after which a spectrophotometric analysis similar to Hansen and Koroleff (1999) was used for the determination of BSi_{SED} concentrations.

2.5 Statistical analysis

The effects of nutrient ratio on the elemental stoichiometry of sinking particulate matter were tested using the *Student´s t-test*. Similarly, the effects of nutrient uptake on POC export rates to the sediment traps were also tested using the *Student´s t-test*. An *F-test two sample for variances* was used to assess homogeneity of variance. Descriptive statistics (*Curtosis-skewness-mean and median*) were applied to check if data distribution was approximately normally. If not normally distributed, data were log transformed and tested for normality and homogeneity again, before running the *Student t-test*. All statistical analyses were conducted using Microsoft Excel 2010, using a significance level of $p<0.05$.

3. Results

3.1 Water column properties

Both OMZ water masses showed similar $Si(OH)_4^-$ and PO_4^{3-} concentrations, but DIN concentration in the low N:P water mass was ~14-fold higher than that of the very low N:P water mass. N:P ratios were 0.11 and more than 15 times that for the very low and low N:P water mass, respectively (Table 3.1).

Table 3.1: Dissolved inorganic nutrient properties of the two OMZ derived water masses. Note that N is the sum of NO_2^-, NO_3^- and NH_4^+ concentrations.

Water mass	$Si(OH)_4^-$ (µmol L^{-1})	N (µmol L^{-1})	PO_4^{3-} (µmol L^{-1})	N:P
Very low N:P	17.437	0.294	2.558	0.11
Low N:P	19.557	4.261	2.492	1.71

Both treatments for all nutrient species were remarkably similar throughout the entire experimental period (Fig. 3.1). However, mean NO_2^- concentrations in the low N:P treatment increased after OMZ water additions. NO_2^-, NO_3^-, NH_4^+ concentrations, in the very low/low N:P mesocosms started at 0.78/1.14, 5.68/5.98, 3.50/4.17 µmol L^{-1} and became depleted on day 26, 24, 18, respectively. A slight increase in NO_2^- and NH_4^+ was observed towards the end of the experiment. Neither, PO_4^{3-} nor $Si(OH)_4^-$ became depleted at any point throughout the experiment (Fig. 3.1). No statistically significant differences were found between treatments in any of the nutrient species (Table 3.2).

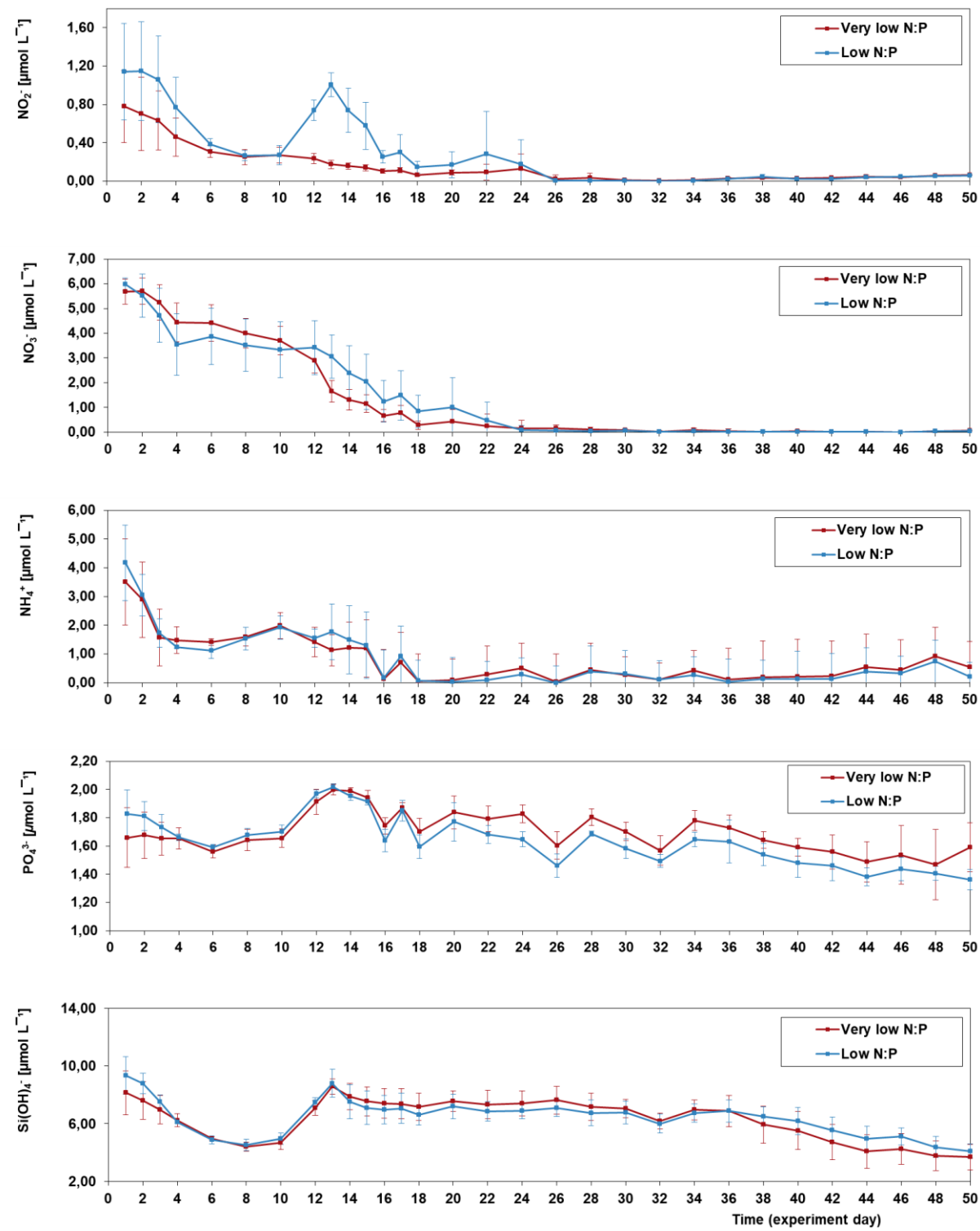

Figure 3.1: Depth integrated mean dissolved inorganic nutrient concentrations of each experimental treatment (n=4). Error bars represent standard deviations of four replicates.

N:P ratios were initially 6.0 and 6.2 (very low and low N:P treatment, respectively), decreased relatively constantly and reached close to zero values at day 18 (Fig. 3.2). Little change was observed thereafter. No significant difference between the two treatments was found (Table 3.2).

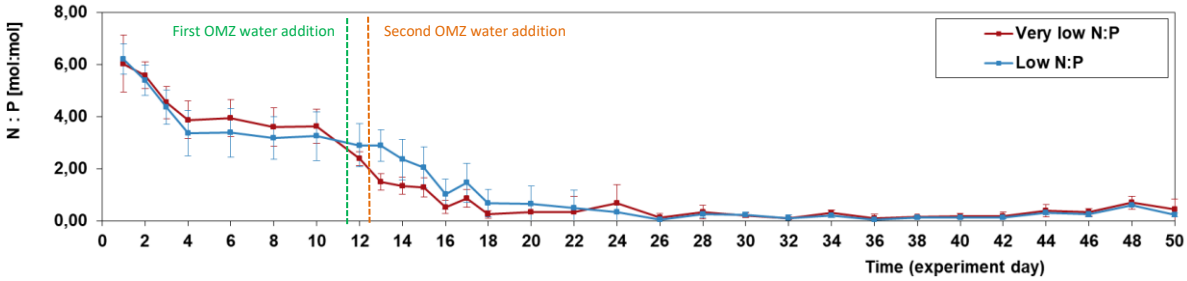

Figure 3.2: Depth integrated mean dissolved inorganic N:P ratio of the treatments (n=4). Error bars represent standard deviations of four replicates. Note that N is the sum of NO_2^-, NO_3^- and NH_4^+ concentrations. First OMZ water addition to the bottom layer of the mesocosms between sampling of day 11 and 12. Second OMZ water additions to the surface layer of the mesocosms between sampling of day 12 and 13.

Table 3.2: Output of the Student´s t-test run in Microsoft Excel 2010, for the entire experimental period. A significance threshold of $p < 0.05$ was used. Note that N:P in the water column refers to dissolved inorganic N:P.

Water column		***Sediment traps***					
	p		**p**		**p**		**p**
NO_2^-	0.35	TPC_{SED}	0.36	C : N	0.68	Cum TPC_{SED}	0.57
NO_3^-	0.82	TPN_{SED}	0.38	C : P	0.27	Cum TPN_{SED}	0.57
NH_4^+	0.35	POC_{SED}	0.38	N : P	0.29	Cum POC_{SED}	0.53
PO_4^{3-}	0.22	PON_{SED}	0.43	PIC : POC	0.31	Cum PON_{SED}	0.72
$Si(OH)_4^-$	0.75	PIC_{SED}	0.59	Σ POC_{SED} $N_{utilized}^{-1}$	0.23	Cum POP_{SED}	0.92
Chl *a*	0.08	POP_{SED}	0.85			Cum BSi_{SED}	0.55
N:P	0.86	BSi_{SED}	0.82				

Chl *a* at the experiment start ranged between 5.2 and 6.6 µg L^{-1} (low/very low N:P) and remained rather constant in both treatments, until they increased markedly towards the end of the experiment, reaching maximum values of 14.7/23.4 µg L^{-1} (very low/low N:P) on day 50 (Fig. 3.3). Chl *a* was not significantly different between treatments (Table 3.2).

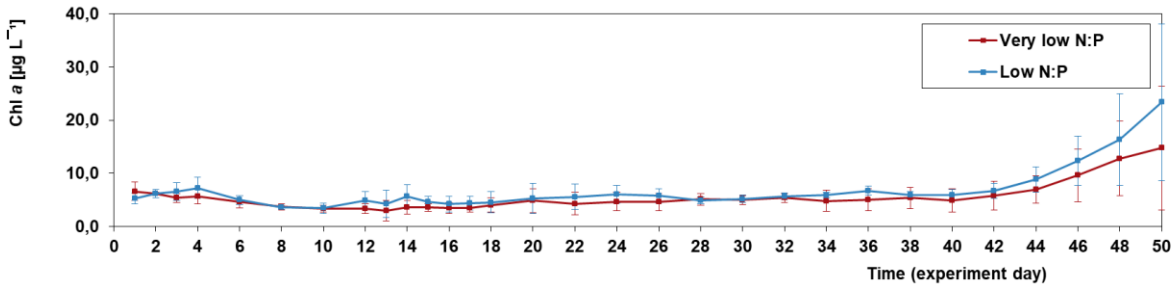

Figure 3.3: Depth integrated mean chlorophyll a concentrations in the water column for each treatment (n=4). Error bars represent standard deviations of four replicates.

3.2 Sediment trap accumulated material and vertical fluxes

The fluxes of all parameters increased over the first eight days, followed by a large drop at day 10 (Fig. 3.4). Maximum fluxes for TPC_{SED}, TPN_{SED}, POC_{SED}, PON_{SED}, PIC_{SED} and Bsi_{SED} were reached on day 12 or 14, shortly after OMZ water additions. POP_{SED} fluxes reached maximum values of 0.31/0.26 µmol L^{-1} $48h^{-1}$ (very low N:P/low N:P) on day 48, although there was another temporal maximum around days 12 to 14. TPC_{SED}, TPN_{SED}, POC_{SED} and PON_{SED} fluxes decreased after OMZ water additions from day 14 to 16 and stayed relatively constant until they increased again towards the end of the experiment. BSi_{SED} fluxes declined continuously after reaching maximum values on days 12 to 14. Close to zero values were observed from day 28 onwards. POC_{SED} and PON_{SED} represented >95% of TPC_{SED} and TPN_{SED}, respectively, with some exceptions. None of the parameters were significantly different between treatments (Table 3.2).

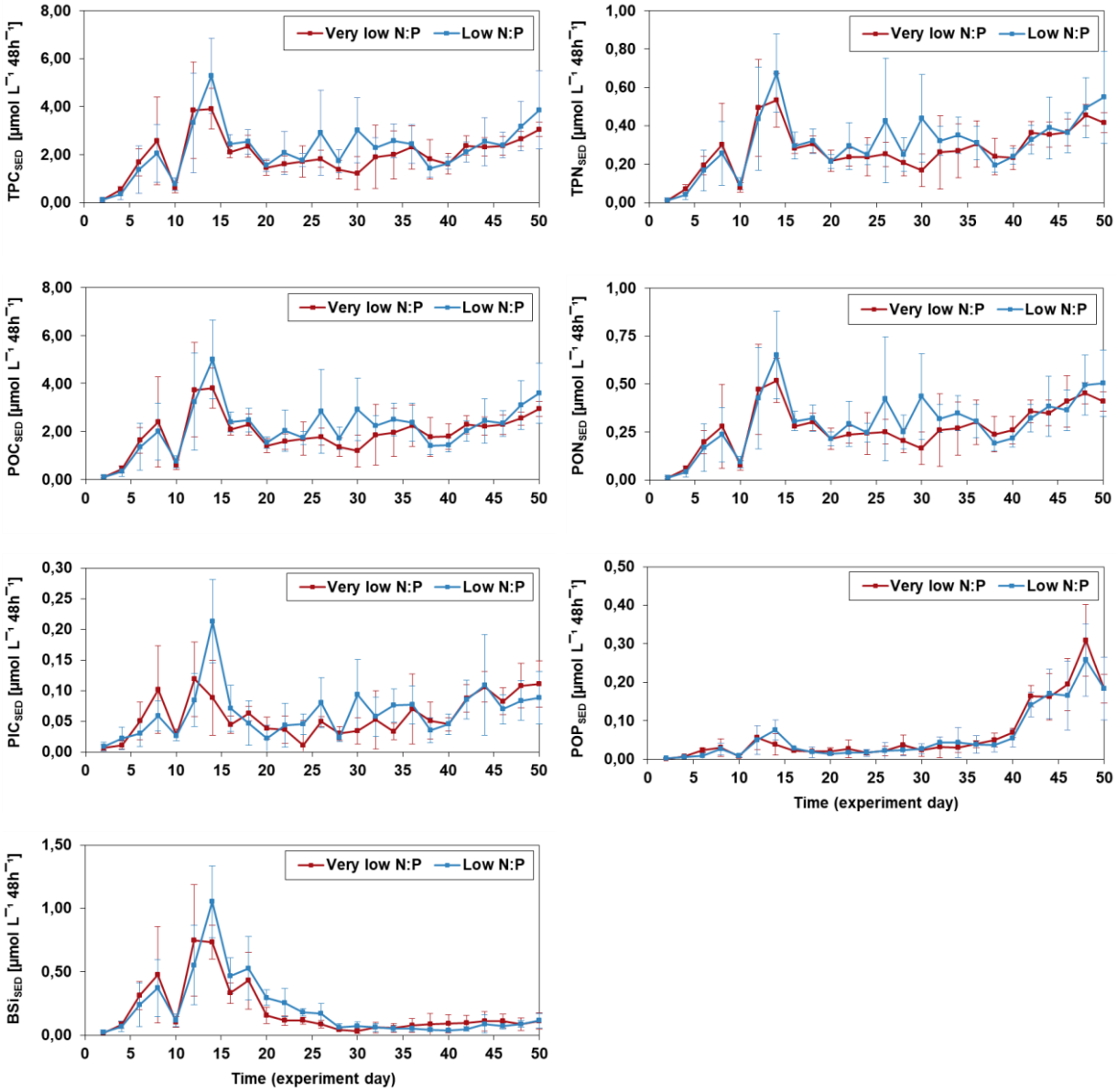

Figure 3.4: Mean fluxes of particulate matter to the sediment traps for the two experimental treatments (n=4). Error bars represent standard deviations of four replicates.

Elevated C:N ratios, compared to the Redfield ratio, for both treatments were observed for almost the entire course of the experiment (Fig. 3.5). A more pronounce decrease in C:N ratios was evident from day 36 onwards, reaching slightly lower than Redfield C:N ratios towards the end of the experiment. C:P and N:P ratios for both treatments stayed mostly below the Redfield ratio of 106 and 16, respectively (Fig. 3.5). Increasing C:P and N:P ratios

were observed towards the middle of the experiment, followed by a decline from day 34 onwards. Mean C:P and N:P values within the last ten days of the experiment dropped to values as low as 9.1/12.7 (very low/low N:P) and 1.6/2.0 (very low/low N:P), respectively. Mean PIC:POC values for both treatments stayed relatively constant after a decrease within the first four to six days (Fig. 3.5). PIC:POC ratios for both treatments were always below 0.08. No significant differences between treatments in any of the ratios were observed (Table 3.2).

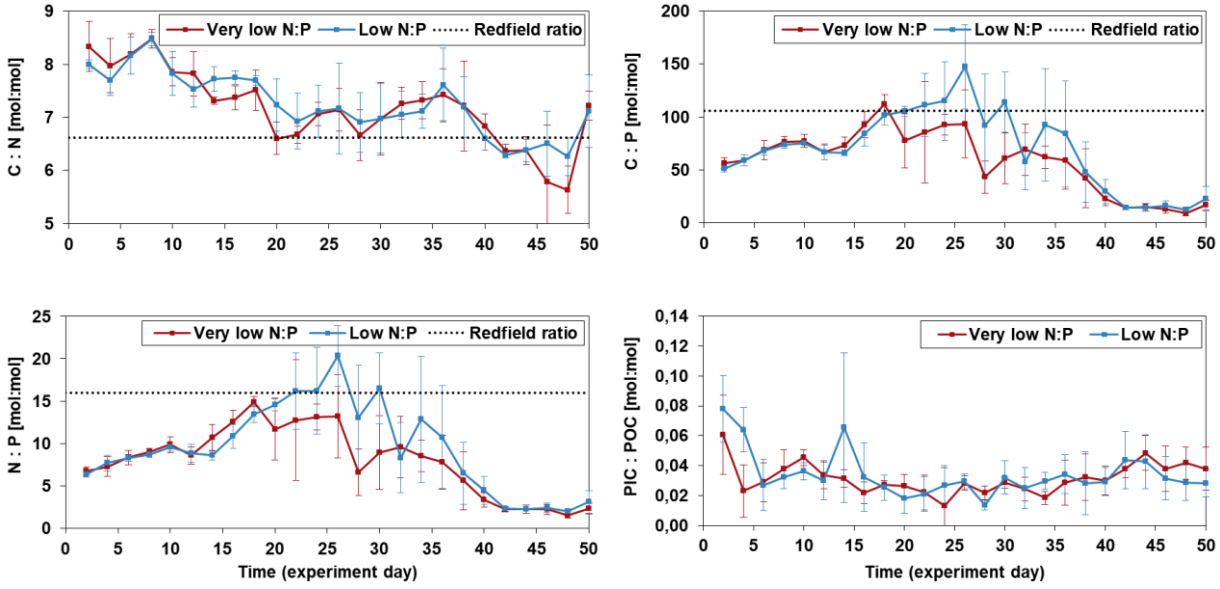

Figure 3.5: Development of mean elemental POM ratios and PIC:POC ratio of particulate matter accumulated into the sediment traps (n=4). Error bars represent standard deviations of four replicates. Note that C:N=POC:PON, C:P=POC:POP and N:P=PON:POP.

Cumulative fluxes to the sediment trap for TPC, TPN, POC and PON showed a constant increase over time for both experimental treatments (Fig.13). These fluxes became slightly higher in the low N:P treatment starting on day 26. Similarly, cumulative POP sediment trap fluxes over time increased gradually for the first 40 days in both treatments, but the accumulation rate increased substantially from day 40 onwards (Fig. 3.6). Opposite to that,

there was a more intense increase for the initial 18 days in cumulative BSi sediment trap fluxes in both treatments, while accumulation ceased thereafter (Fig. 3.6). Additionally, once the accumulation declined after day 18, fluxes in the low N:P treatment were slightly higher, compared to the very low N:P treatment. No statistically significant differences between treatments for any of the parameters were found (Table 3.2).

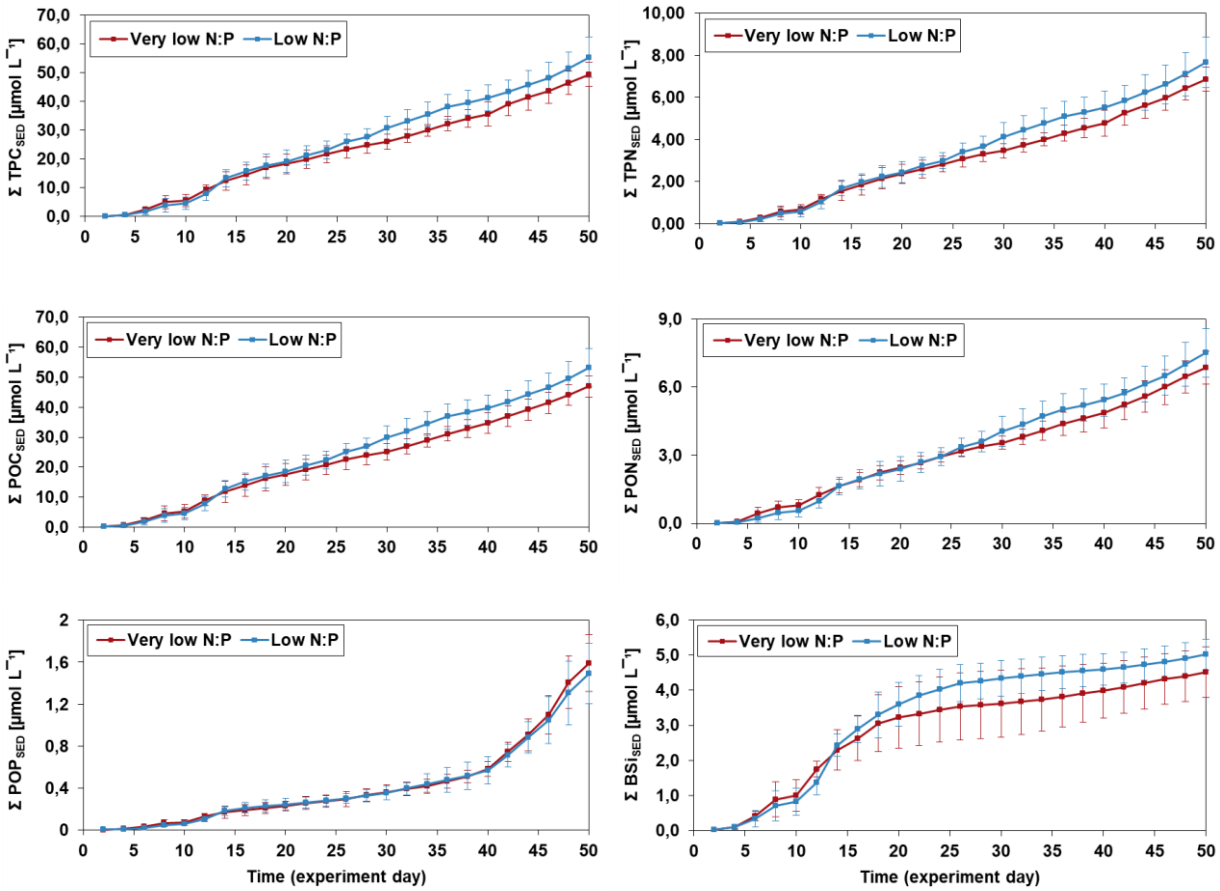

Figure 3.6: Mean cumulative particulate matter collected in the sediment traps (n=4). Error bars represent standard deviations of four replicates.

Total export of POC to the sediment traps per utilized dissolved inorganic N in the water column was 8.97 and 4.91 for the very low and low N:P treatment, respectively (Fig. 3.7). Statistically, the difference between the two treatments was not significant (Table 3.2), although their average value was markedly different (Fig. 3.7). Even though more DIN was

used under the low N:P mesocosms compared to the very low N:P mesocosms (appendix Table 6.2), POC export per utilized N in the water column was lower (Fig. 3.7). Interestingly, the reason as to why the treatments seem different, with respect to this parameter, is mesocosm 4 having a much higher value compared to all other mesocosms (appendix Fig. 6.3).

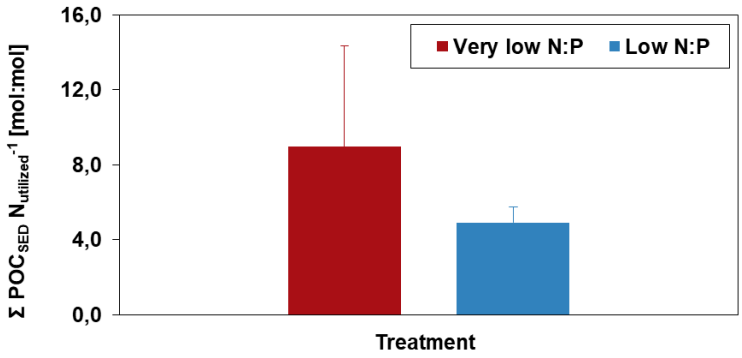

Figure 3.7: Mean total POC export to sediment traps per utilized N in the water column (n=4). Error bars represent standard deviations of four replicates. deviation.

4. Discussion

Since there have been no statistically significant differences in any of the parameters between the two experimental treatments, this discussion will mainly focus on the observed trends of the treatments over time. Furthermore, possible explanations as to why there have not been any statistically significant differences between the treatments will be discussed.

4.1 How accurate was upwelling simulation?

Simulated upwelling using water masses with different dissolved inorganic N:P ratios did not lead to changes in the elemental stoichiometry of sinking particulate matter (Table. 1). This is likely due to the fact, that the dissolved inorganic N:P ratio in the mesocosms, throughout the entire experimental period, also did not differ significantly, even though the OMZ water added to the low N:P mesocosms showed a dissolved inorganic N:P ratio 15-fold higher than the very low N:P treatment (Table 3.1). The proportion of dissolved inorganic N to P in seawater may promote particular plankton communities, with certain biogeochemical consequences, based on the species specific metabolic requirements (Deutsch and Weber, 2012). Both treatments reached close to zero values in these dissolved inorganic nutrient proportions shortly after OMZ water additions, most likely due to phytoplankton removing reactive N from the water. This finding is supported by decreasing concentrations of NO_3^- (and NO_2^-) after OMZ water additions (Fig. 3.1), probably making N the limiting nutrient for phytoplankton growth, since P in the mesocosms was available in high concentrations throughout the entire experiment. DIN concentrations below 1 µM and dissolved inorganic N:P ratios below 10 have been attributed to nitrogen limitation (Dortch and Whitledge,

1992). However, it has been shown that *in situ* concentrations and ratios of nutrients may not suffice in evaluating the occurrence of nutrient limitation of phytoplankton growth (Domingues et al., 2017).

It is important to not only look at nutrient stoichiometry but also address absolute concentrations of nutrients, especially in the OMZ derived water masses. Nutrient concentration also influences plankton community composition, since small phytoplankton taxa may outcompete larger cells under nutrient scarce conditions (Franz et al., 2012b). The observed concentrations of dissolved inorganic nitrogen species in the retrieved OMZ water masses, especially nitrate, were much lower than expected, even for an OMZ influenced upwelling event (appendix Table 6.1). Indeed, Franz et al. (2012b) reported nitrate concentrations over 25 µmol L^{-1} over the shallow Peruvian coastal waters (<100m). However, the added water masses in this experiment were retrieved very close to the seafloor. Therefore, dissolved inorganic N concentrations of the collected water masses may also have been reduced due to the coupling between sediments and overlying water. Sediments can act as sources or sinks for nutrients, and biogeochemical processes occurring within the sediment and the pelagic zone are closely coupled (McGlathery et al., 2004). Nutrient fluxes at the sediment-water interface in coastal oceans are important processes affecting the chemical composition of the overlying water, ultimately influencing primary productivity (Callender and Hammond, 1982). Variations in physical-chemical factors and hydrodynamic disturbances may lead to a release of nutrients from the sediment to the overlying water (Yang et al., 2017). Dissolved inorganic N:P ratios lower than the Redfield ratio of 16:1 (Redfield, 1958) have been reported in coastal waters of the Eastern Tropical North Atlantic as a result of benthic N-loss to and P release from the sediment (Meyer et al.,

2016). Furthermore, chemical nutrient conditions of the two OMZ water masses mostly were very similar to each other (Table 3.1 and 3). This may largely explain why the treatments were not significantly different from one another.

As can be seen in Figure 15 (appendix), dissolved oxygen concentration inside all mesocosms decreased rapidly with depth below 5m, but oxic conditions were observed for most of the water column. Decreasing oxygen concentrations have been correlated with increasing denitrification rates (Gruber, 2008), a process commonly associated with nitrogen losses in OMZs. However, low concentrations of NO_3^- and NH_4^+ may indicate anammox activity in suboxic waters (Arrigo, 2005), a process related to nitrogen loss over the Benguela OMZ (Kuypers et al., 2005).

4.2 Water column properties

In order to ensure optimal starting conditions for the experiment, similarity in chemical and biological conditions between mesocosm bags after closure is desired (Riebesell et al., 2013). However, initial concentrations of dissolved inorganic nutrients varied across mesocosms, especially for NO_2^- and NH_4^+ (appendix Table 6.3). It is notable that lowest values for all variables were observed in mesocosm 4 (M4). This information can be used to explain the remarkably different behaviour of M4 during parts of the experimental period, for some variables (see below).

Chl *a* ranged between 3.0 and 7.0 µg L^{-1} for the first 40 days of the experiment, in both treatments, despite the depletion in all dissolved inorganic nitrogen species after day 18. Therefore, since Chl *a* did not decrease, phytoplankton biomass was probably supported by

other sources, including remineralized PON/DON or direct DON uptake. Remineralisation of PON and DON increases the concentration of dissolved inorganic nutrients (Gruber, 2008), but no visible subsequent increase in any of the dissolved inorganic nitrogen species was observed immediately after their depletion (Fig. 3.1). This fact could reflect a fast incorporation of remineralized N by phytoplankton, as soon as it was made available. The relatively low sampling frequency, with a long 48h period between successive sampling stages, only allowed a glimpse of the "bigger picture", not evaluating short-term processes of nutrient production and use. Additionally, it has been hypothesized that excess phosphate favours increased rates of N_2-fixation by diazotrophs (Deutsch et al., 2007; Meyer et al., 2016). Phosphate has been present for the whole course of the experiment (Fig. 3.1), but data on organic nitrogen in the water column is needed, in order to make more accurate inferences. Microzooplankton as consumers of phytoplankton (mostly protists), may have also had a relevant role in remineralization processes, through excretion of inorganic nutrients and introduction of fecal pellets into the POM pool (Calbet and Landry, 2004; Turner, 2015). Enhanced remineralization of phosphate and ammonium has been observed in the presence of microzooplankton (Le Moigne et al., 2013).

Previous studies have shown that DON compounds (e.g., urea), that usually represent the largest pool of bioavailable N in most aquatic systems (Bronk et al., 2007), can be a viable direct source of reactive N to phytoplankton, particularly when competing for limited dissolved inorganic N with heterotrophic prokaryotes (Berman et al., 1999; Bradley et al., 2010; Bronk et al., 2007). Furthermore, it is likely that the phytoplankton assemblage in the second half of the experiment was dominated by organisms other than diatoms, since BSi_{SED} fluxes were almost non-existent.

The direct ingestion of living prey by mixotrophic phytoplankton could also explain the continuous increase in Chl *a* during the second half of the experiment, under reduced nutrient conditions. According to the review of Stoecker et al. (2017), mixotrophic phytoplankton, including dinoflagellates and nanoflagellates, are ubiquitous in coastal oceans and are associated with upwelling zones. For these phagotrophic organisms, dissolved inorganic nutrient acquisition is supplemented or substituted by the ingestion of prey. Additionally, mixotrophy may also stimulate vertical carbon export through a more efficient transfer of organic matter into larger plankton, ultimately improving the efficiency of the biological carbon pump (Hammer and Pitchford, 2006; Stoecker et al., 2017).

4.3 Elemental stoichiometry of sinking particulate matter

The proportion of particulate organic carbon to nitrogen (C:N ratio) is of fundamental importance in ocean biogeochemistry, as it relates to the efficiency of carbon sequestration, secondary production and the biological pump. It also holds valuable information for the coupling between the carbon and nitrogen cycles (Martiny et al., 2013a and b; Sterner et al., 2008).

C:N ratios were higher than the Redfield ratio (6.6) for almost the entire experimental period (Fig. 3.5). N limitation and lower dissolved N:P ratios have been linked with high particulate C:N ratios (Martiny et al., 2013b). Since N concentrations in the added water masses in this study were remarkably low for an upwelling event (Franz et al., 2012b), leading to dissolved N:P ratios well below the Redfield ratio, the observed C:N ratio in the sinking particulate matter may be attributed to N limitation, ultimately resulting in a lower nitrogen cell quota for phytoplankton (Martiny et al., 2013b). C:N ratios gradually

decreased, reaching values close to or below the Redfield ratio as the end of the experiment approached (Fig. 3.5), even though DIN concentrations only increased slightly (Fig. 3.1). Additionally, phytoplankton growing under light limitation may accumulate less carbon storage polymers (Martiny et al., 2013b), therefore resulting in a decreased cellular C:N ratio. Biological matter that settled on the outside wall of the mesocosm bags was cleaned regularly, to a depth of approximately 6m. Below that, no cleaning was carried out. Thus, PAR intensity inside the mesocosms showed a substantial decline below 6 m depth level, eventually leading to increased light limitation (appendix Fig. 6.1 top). It could be argued that this gradual decrease of light availability is linked to the relatively constant decrease of C:N, as phytoplankton during the experiment accumulated less and less carbon storage polymers over time.

PIC:POC ratios, often used as a measure of carbon export (Gerecht et al., 2014), stayed relatively constant for the entire experimental period. Decreased PIC:POC ratios are linked to a higher potential for oceanic CO_2 uptake and, therefore, a higher drawdown of atmospheric CO_2 on longer time scales (Fielding, 2014; Gerecht et al., 2014). The PIC:POC ratios observed in this study were very low, staying <0.08 at all times (Findlay et al., 2011; Gerecht et al., 2014). Calcifying phytoplankton (e.g., coccolithophores) fix HCO_3^- into PIC through calcification (i.e., production of calcium carbonate cocccoliths), and into POC through photosynthesis (Bach, 2015; Gerecht et al., 2014; Monteiro et al., 2016). Thus, since PIC_{SED} concentrations were also low (Fig. 3.4), the impact of calcifying organisms on the CO_2 fixation to POC was probably reduced in this study.

Both C:P and N:P ratios were well below the Redfield ratios throughout most of the experimental period (Fig. 3.5). According to Arrigo (2005), the cellular C:P and N:P ratios of

eukaryotic phytoplankton vary markedly between the green and red plastid superfamilies. The red superfamily (ca. C:P =70, N:P = 10) usually exhibits significantly lower ratios than the green superfamily (C:P ~200, N:P ~27). Thus, it can be argued that the observed ratios are the result of phytoplankton assemblages mainly composed by representatives of the red plastid superfamily. Diatoms are included in the red superfamily (Quigg et al., 2003), and the BSi_{SED} concentrations during the first half of the experiment inside the sediment traps, support their presence (Nelson et al., 1995). C:P and N:P lower than Redfield ratios, as observed in this study, have been measured for diatoms (Martiny et al., 2013a). The remarkably low values for the last ~ten days of the experiment probably reflected the steep increase in POP_{SED} during this period (Fig. 3.4). An increase in POP of such magnitude is unexpected and was likely the result of guano deposition by seabirds. Seabird guano, rich in nitrogen and phosphorous, is associated with enhanced phytoplankton productivity and may alter species composition of the phytoplankton community (Bosman and Hockey, 1986; Shatova et al., 2017; Wootton, 1991). Deposition of seabird guano in the Bering Sea was associated with tenfold increases in the uptake of mineral and organic compounds by phytoplankton, as well as peaks in phytoplankton biomass (Wainright et al., 1998). Thus, the remarkably low C:P and N:P ratios in the sediment traps at the end of the experiment may be due to increased phytoplankton biomass. This statement was supported by a steep rise in Chl *a* during the later stage of the experiment. Furthermore, increasing POC and PON fluxes into the sediment traps from day 40 onwards also supported this (Fig. 3.4). Seabirds, particularly inca terns (*Larosterna inca*), were increasingly sighted, sitting on the metal rings and cleats of the mesocosms over the last two weeks of the experiment. We have also observed guano input by inca terns many times. In addition, an increased occurrence of large fish (>10cm) inside the sediment traps was observed from day 34 onwards. Since we

have also seen some inca terns dropping their prey into the mesocosms, this increased observation of fish within the sediment trap material coincided with increased sightings of seabirds on the mesocosms. Fish and fish remains (e.g., bones) were removed from the sediment trap samples to the best of our ability. Whenever there were indications of fish contamination of sediment trap material, the entire material was filtered through a mesh (2mm mesh size), and fish remains were carefully picked out and washed with filtered seawater (0.2µm), in order to minimize sample loss, while maximizing fish removal. Therefore, the increase in particulate matter for the last 10 days was probably associated with the fertilization of mesocosms with guano, and the subsequent stimulation of phytoplankton net growth rate. Efforts to deter seabirds were increased, once they became more abundant, but no satisfying result was achieved as birds kept on coming back to the mesocosms.

4.4 Vertical export

An inverse relationship between export efficiency and primary production (PP) has been observed in multiple studies (Le Moigne et al., 2016; Maiti et al., 2013). If we assume that utilized N is an indicator of total PP, PP was higher in the low N:P mesocosms. M4 showed the lowest Chl *a* for most of the experimental period, supporting this statement (appendix Fig. 6.2). Furthermore, less dissolved inorganic N was apparently used inside M4 (Table 6.2). Therefore, the export efficiency inside M4 was probably higher, in respect to other mesocosms. Potential hypothesis explaining this unexpected relationship include intense surface microbial recycling in high PP areas and grazing-mediated export that varies inversely with PP (Le Moigne et al., 2016). However, caution is advised when comparing

those findings with results of this study, since these studies have been carried out in the Southern Ocean.

Cumulative fluxes of TPC, TPN, POC, PON and BSi into the sediment traps were almost always higher under the low N:P treatment, especially in the second half of the experiment (Fig. 3.6). Even though not significant, this pattern agreed with previous studies that report an increased exportation when nutrient availability and PP are higher (Le Moigne et al., 2016; Haskell, 2015). Since slightly more nutrients (nitrogen in particular) were available and apparently utilized under the low N:P treatment (Table 6.2 and Fig. 3.1), the slightly higher cumulative fluxes of TPC, TPN, POC, PON and BSi into the sediment traps are justified. Higher accumulation rates in cumulative BSi_{SED} fluxes during the beginning of the experiment (Fig. 3.6) were associated with greater BSi_{SED} fluxes at the same time (Fig. 3.4), probably a result of diatom blooms, until dissolved inorganic nitrogen became depleted (Fig. 3.1). Organisms other than diatoms, such as choanoflagellates and radiolaria, may also have contributed to BSi_{SED} fluxes by undergoing biosilicification (Marron et al., 2013). The future evaluation of plankton composition will allow their quantification, if relevant.

4.5 Conclusions and outlook

In this study, water masses with different dissolved inorganic N:P ratios, associated with OMZ influenced upwelling events, were not associated with differences in the elemental stoichiometry of sinking particulate matter. Furthermore, apparent nutrient uptake was not related to differences in POC exportation rates. Our results showed clear deviations from the canonical Redfield ratio in sinking POM, hypothesized to be related with phytoplankton community composition. Quantitative data on phytoplankton composition, which will be

made available in the next months (after the deadline of this master thesis), should be used for testing this hypothesis. Sinking POM is partly composed of zooplankton fecal pellets and the vertical export of particulate matter is, to some extent, influenced by active zooplankton migration. Therefore, the influence of zooplankton on elemental stoichiometries of sinking particulate matter should be further considered.

Furthermore, the potential importance of DON as source of N for phytoplankton, as well as the ingestion of living prey, must be assessed. Thus, once community data is available, the occurrence of mixotrophic phytoplankton taxa should be specifically evaluated. Additionally, DON concentrations could help to shed light on the nutritional source for phytoplankton (DON data will also only be made available after the deadline of this thesis).

Potential issues during this experimental study included seabird disturbances (e.g., guano and prey input). In regions with high seabird abundances, a more effective strategy to deter seabirds from the mesocosms should be applied, such as spanning a thin net layer between the mesocosm roof and metal rings. Since this would greatly impede and slow down sampling procedures, such a net should be limited to sites of the mesocosms where no sampling is carried out. Furthermore, the net should be thin, with a relatively large mesh size, in order to minimize its impact on PAR entering the mesocosms. Since the two added OMZ derived water masses were remarkably similar to each other, also chemical and biological parameters throughout the experiment were relatively similar to each other. A second OMZ water collection and addition was planned to be carried out, but could not be realized, due to technical difficulties.

The ocean´s ability to transfer carbon away from the surface to the deep ocean is of fundamental importance in reducing CO_2 in the atmosphere, without which, accelerated

atmospheric CO_2 growth would be observed, since more anthropogenic CO_2 would remain in the atmosphere (Le Moigne et al., 2013; Le Quéré et al., 2010). Therefore, biogeochemical processes that alter carbon export or elemental stoichiometries are important aspects in changing ocean environments and must be discussed, in order to understand the coupling between these processes.

5. References

Aigars, J., Poikāne, R., Dalsgaard, T., Eglīte, E. and Jansons, M. (2015). Biogeochemistry of N, P and SI in the Gulf of Riga surface sediments: Implications of seasonally changing factors. *Continental Shelf Research*, 105, pp.112-120.

Agusti, S., González-Gordillo, J., Vaqué, D., Estrada, M., Cerezo, M., Salazar, G., Gasol, J. and Duarte, C. (2015). Ubiquitous healthy diatoms in the deep sea confirm deep carbon injection by the biological pump. *Nature Communications*, 6, p.7608.

Arrigo, K. (2005). Marine microorganisms and global nutrient cycles. *Nature*, 437(7057), pp.349-355.

Arístegui, J., Gasol, J., Duarte, C. and Herndld, G. (2009). Microbial oceanography of the dark ocean's pelagic realm. *Limnology and Oceanography*, 54(5), pp.1501-1529.

Bach, L. (2015). Reconsidering the role of carbonate ion concentration in calcification by marine organisms. *Biogeosciences*, 12(16), pp.4939-4951.

Bakun, A., 1990. Global climate change and instensification of coastal ocean upwelling. *Science*, 247(4939), pp.198–201.

Bakun, A. and Weeks, S. (2008). The marine ecosystem off Peru: What are the secrets of its fishery productivity and what might its future hold?. *Progress in Oceanography*, 79(2-4), pp.290-299.

Berman, T., Béchemin, C. and Maestrini, S. (1999). Release of ammonium and urea from dissolved organic nitrogen in aquatic ecosystems. *Aquatic Microbial Ecology*, 16, pp.295-302.

Bohlen, L., Dale, A., Sommer, S., Mosch, T., Hensen, C., Noffke, A., Scholz, F. and Wallmann, K. (2011). Benthic nitrogen cycling traversing the Peruvian oxygen minimum zone. *Geochimica et Cosmochimica Acta*, 75(20), pp.6094-6111.

Bosman, A. and Hockey, P. (1986). Seabird guano as a determinant of rocky intertidal community structure. *Marine Ecology Progress Series*, 32, pp.247-257.

Boxhammer, T., Bach, L., Czerny, J. and Riebesell, U. (2015). Technical Note: Sampling and processing of mesocosm sediment trap material for quantitative biogeochemical analysis. *Biogeosciences Discussions*, 12(22), pp.18693-18722.

Bradley, P., Sanderson, M., Frischer, M., Brofft, J., Booth, M., Kerkhof, L. and Bronk, D. (2010). Inorganic and organic nitrogen uptake by phytoplankton and heterotrophic bacteria in the stratified Mid-Atlantic Bight. *Estuarine, Coastal and Shelf Science*, 88(4), pp.429-441.

Brandes, J., Devol, A. and Deutsch, C. (2007). New Developments in the Marine Nitrogen Cycle. *Chemical Reviews*, 107(2), pp.577-589.

Bronk, D., See, J., Bradley, P. and Killberg, L. (2007). DON as a source of bioavailable nitrogen for phytoplankton. *Biogeosciences*, 4(3), pp.283-296.

Bruland, K., Rue, E., Smith, G. and DiTullio, G. (2005). Iron, macronutrients and diatom blooms in the Peru upwelling regime: brown and blue waters of Peru. *Marine Chemistry*, 93(2-4), pp.81-103.

Caddy, J. and Bakun, A. (1994). A tentative classification of coastal marine ecosystems based on dominant processes of nutrient supply. *Ocean & Coastal Management*, 23(3), pp.201-211.

Calbet, A. and Landry, M. (2004). Phytoplankton growth, microzooplankton grazing, and carbon cycling in marine systems. *Limnology and Oceanography*, 49(1), pp.51-57.

Callender, E. and Hammond, D. (1982). Nutrient exchange across the sediment-water interface in the Potomac River estuary. *Estuarine, Coastal and Shelf Science*, 15(4), pp.395-413.

Capone, D. and Hutchins, D. (2013). Microbial biogeochemistry of coastal upwelling regimes in a changing ocean. *Nature Geoscience*, 6(9), pp.711-717.

Czerny, J., Schulz, K., Krug, S., Ludwig, A. and Riebesell, U. (2013). Technical Note: The determination of enclosed water volume in large flexible-wall mesocosms "KOSMOS." *Biogeosciences*, 10(3), pp.1937-1941.

Daneri, G., Dellarossa, V., Quiñones, R., Jacob, B., Montero, P. and Ulloa, O. (2000). Primary production and community respiration in the Humboldt Current System off Chile and associated oceanic areas. *Marine Ecology Progress Series*, 197, pp.41-49.

Deutsch, C., Sarmiento, J., Sigman, D., Gruber, N. and Dunne, J. (2007). Spatial coupling of nitrogen inputs and losses in the ocean. *Nature*, 445(7124), pp.163-167.

Deutsch, C. and Weber, T. (2012). Nutrient Ratios as a Tracer and Driver of Ocean Biogeochemistry. *Annual Review of Marine Science*, 4(1), pp.113-141.

Domingues, R., Guerra, C., Barbosa, A. and Galvão, H. (2017). Will nutrient and light limitation prevent eutrophication in an anthropogenically-impacted coastal lagoon?. *Continental Shelf Research*, 141, pp.11-25.

Dortch, Q. and Whitledge, T. (1992). Does nitrogen or silicon limit phytoplankton production in the Mississippi River plume and nearby regions?. *Continental Shelf Research*, 12(11), pp.1293-1309.

Elser, J., Bracken, M., Cleland, E., Gruner, D., Harpole, W., Hillebrand, H., Ngai, J., Seabloom, E., Shurin, J. and Smith, J. (2007). Global analysis of nitrogen and phosphorus limitation of primary producers in freshwater, marine and terrestrial ecosystems. *Ecology Letters*, 10(12), pp.1135-1142.

Fielding, S. (2014). Predicting coccolithophore rain ratio responses to calcite saturation state. *Marine Ecology Progress Series*, 500, pp.57-65.

Filippelli, G. (2001). Carbon and phosphorus cycling in anoxic sediments of the Saanich Inlet, British Columbia. *Marine Geology*, 174(1-4), pp.307-321.

Findlay, H., Calosi, P. and Crawfurd, K. (2011). Determinants of the PIC : POC response in the coccolithophore Emiliania huxleyi under future ocean acidification scenarios. *Limnology and Oceanography*, 56(3), pp.1168-1178.

Föllmi, K. (1996). The phosphorus cycle, phosphogenesis and marine phosphate-rich deposits. *Earth-Science Reviews*, 40(1-2), pp.55-124.

Franz, J., Hauss, H., Sommer, U., Dittmar, T. and Riebesell, U. (2012a). Production, partitioning and stoichiometry of organic matter under variable nutrient supply during mesocosm experiments in the tropical Pacific and Atlantic Ocean. *Biogeosciences*, 9(11), pp.4629-4643.

Franz, J., Krahmann, G., Lavik, G., Grasse, P., Dittmar, T. and Riebesell, U. (2012b). Dynamics and stoichiometry of nutrients and phytoplankton in waters influenced by the oxygen minimum zone in the eastern tropical Pacific. *Deep Sea Research Part I: Oceanographic Research Papers*, 62, pp.20-31.

Froelich, P., Bender, M. and Luedtke, N. (1982). The marine phosphorous cycle. *American Journal of Science*, 282, pp.474–511.

Fuenzalida, R., Schneider, W., Garcés-Vargas, J., Bravo, L. and Lange, C. (2009). Vertical and horizontal extension of the oxygen minimum zone in the eastern South Pacific Ocean. *Deep Sea Research Part II*, 56(16), pp.992-1003.

Gerecht, A., Šupraha, L., Edvardsen, B., Probert, I. and Henderiks, J. (2014). High temperature decreases the PIC/POC ratio and increases phosphorus requirements in Coccolithus pelagicus (Haptophyta). *Biogeosciences*, 11(13), pp.3531–3545.

Gervais, F. and Riebesell, U. (2001). Effect of phosphorus limitation on elemental composition and stable carbon isotope fractionation in a marine diatom growing under different CO2 concentrations. *Limnology and Oceanography*, 46(3), pp.497-504.

Giblin, A., Tobias, C., Song, B., Weston, N., Banta, G. and Rivera-Monroy, V. (2013). The Importance of Dissimilatory Nitrate Reduction to Ammonium (DNRA) in the Nitrogen Cycle of Coastal Ecosystems. *Oceanography*, 26(3), pp.124-131.

Gier, J., Sommer, S., Löscher, C., Dale, A., Schmitz, R. and Treude, T. (2016). Nitrogen fixation in sediments along a depth transect through the Peruvian oxygen minimum zone. *Biogeosciences*, 13(14), pp.4065-4080.

Glock, N., Schönfeld, J., Eisenhauer, A., Hensen, C., Mallon, J. and Sommer, S. (2013). The role of benthic foraminifera in the benthic nitrogen cycle of the Peruvian oxygen minimum zone. *Biogeosciences Discussions*, 9(12), pp.17775-17817.

Gomez, E., Durillon, C., Rofes, G. and Picot, B. (1999). Phosphate adsorption and release from sediments of brackish lagoons: pH, O2 and loading influence. *Water Research*, 33(10), pp.2437-2447.

Gruber, N. (2008). The Marine Nitrogen Cycle: Overview and Challenges. In: D. Capone, D. Bronk, M. Mulholland and E. Carpenter, ed., *Nitrogen in the Marine Environment*, 2nd ed. Elsevier, pp.1-43.

Hammer, A. and Pitchford, J. (2006). Mixotrophy, allelopathy and the population dynamics of phagotrophic algae (cryptophytes) in the Darss Zingst Bodden estuary, southern Baltic. *Marine Ecology Progress Series*, 328, pp.105-115.

Han, C., Ren, J., Wang, Z., Tang, H. and Xu, D. (n.d.). A novel hybrid sensor for combined imaging of dissolved oxygen and labile phosphorus flux in sediment and water. *Water Research*, 108, pp.179-188.

Hansen, H. P., and Koroleff, F. (1999). Determination of nutrients. In: K. Grasshoff, K. Kremling and M. Ehrhardt, ed., *Methods of Seawater Analysis*, Wiley-VCH Verlag GmbH, pp.159–228.

Haskell, W. (2015). *Ecosystem export efficiency in an upwelling region: A two-year time series study of vertical transport, particle export and in-situ net and gross oxygen production*. Ph.D. University of Southern California.

Hauss, H., Franz, J. and Sommer, U. (2012). Changes in N:P stoichiometry influence taxonomic composition and nutritional quality of phytoplankton in the Peruvian upwelling. *Journal of Sea Research*, 73, pp.74-85.

Hydes, D., Aoyama, M., Aminot, A., Bakker, K., Becker, S., Coverly, S., Daniel, A., Dickson, A., Grosso, O., Kerouel, R., van Ooijen, J., Sato, K., Tanua, T., Woodward, E. and Zhang, J. (2010). *Determination of dissolved nutrients (N, P, Si) in seawater with high precision and inter-comparability using gas-segmented continuous flow analysers*. In The GO-SHIP Repeat Hydrography Manual : A Collection of Expert Reports and guidelines. IOCCP Report No 14, ICPO Publication Series No. 134, version 1, 2010 (UNESCO/IOC), pp.1-87.

Kalvelage, T., Lavik, G., Lam, P., Contreras, S., Arteaga, L., Löscher, C., Oschlies, A., Paulmier, A., Stramma, L. and Kuypers, M. (2013). Nitrogen cycling driven by organic matter export in the South Pacific oxygen minimum zone. *Nature Geoscience*, 6(3), pp.228-234.

Kérouel, R. and Aminot, A. (1997). Fluorometric determination of ammonia in sea and estuarine waters by direct segmented flow analysis. *Marine Chemistry*, 57(3-4), pp.265-275.

Klausmeier, C., Litchman, E., Daufresne, T. and Levin, S. (2004). Optimal nitrogen-to-phosphorus stoichiometry of phytoplankton. *Nature*, 429(6988), pp.171-174.

Kristensen, E. (2000). Organic matter diagenesis at the oxic/anoxic interface in coastal marine sediments, with emphasis on the role of burrowing animals. *Hydrobiologia*, 426(1), pp.1-24.

Kuypers, M., Lavik, G., Woebken, D., Schmid, M., Fuchs, B., Amann, R., Jorgensen, B. and Jetten, M. (2005). Massive nitrogen loss from the Benguela upwelling system through anaerobic ammonium oxidation. *Proceedings of the National Academy of Sciences*, 102(18), pp.6478-6483.

Lachkar, Z., Smith, S., Lévy, M. and Pauluis, O. (2016). Eddies reduce denitrification and compress habitats in the Arabian Sea. *Geophysical Research Letters*, 43(17), pp.9148-9156.

Lam, P. and Kuypers, M. (2011). Microbial Nitrogen Cycling Processes in Oxygen Minimum Zones. *Annual Review of Marine Science*, 3(1), pp.317-345.

Lam, P., Lavik, G., Jensen, M., van de Vossenberg, J., Schmid, M., Woebken, D., Gutierrez, D., Amann, R., Jetten, M. and Kuypers, M. (2009). Revising the nitrogen cycle in the Peruvian oxygen minimum zone. *Proceedings of the National Academy of Sciences*, 106(12), pp.4752-4757.

Le Moigne, F., Gallinari, M., Laurenceau, E. and De La Rocha, C. (2013). Enhanced rates of particulate organic matter remineralization by microzooplankton are diminished by added ballast minerals. *Biogeosciences*, 10(9), pp.5755-5765.

Le Moigne, F., Henson, S., Cavan, E., Georges, C., Pabortsava, K., Achterberg, E., Ceballos-Romero, E., Zubkov, M. and Sanders, R. (2016). What causes the inverse relationship between primary production and export efficiency in the Southern Ocean?. *Geophysical Research Letters*, 43(9), pp.4457-4466.

Le Moigne, F., Poulton, A., Henson, S., Daniels, C., Fragoso, G., Mitchell, E., Richier, S., Russell, B., Smith, H., Tarling, G., Young, J. and Zubkov, M. (2015). Carbon export efficiency and phytoplankton community composition in the Atlantic sector of the Arctic Ocean. *Journal of Geophysical Research: Oceans*, 120(6), pp.3896-3912.

Le Quéré, C., Takahashi, T., Buitenhuis, E., Rödenbeck, C. and Sutherland, S. (2010). Impact of climate change and variability on the global oceanic sink of CO2. *Global Biogeochemical Cycles*, 24, GB4007.

Marron, A., Alston, M., Heavens, D., Akam, M., Caccamo, M., Holland, P. and Walker, G. (2013). A family of diatom-like silicon transporters in the siliceous loricate choanoflagellates. *Proceedings of the Royal Society B: Biological Sciences*, 280(1756), 20122543.

Monteiro, F., Bach, L., Brownlee, C., Bown, P., Rickaby, R., Poulton, A., Tyrrell, T., Beaufort, L., Dutkiewicz, S., Gibbs, S., Gutowska, M., Lee, R., Riebesell, U., Young, J. and Ridgwell, A. (2016). Why marine phytoplankton calcify. *Science Advances*, 2(7), e1501822.

Luis, J.F. (2007). Mirone: A multi-purpose tool for exploring grid data. *Computers and Geosciences*, 33, pp.31-41.

Mackey, M.D., Higgins, H.W., Mackey, D.J., Wright, S.W., 1997. CHEMTAX User's Manual: A Program for Estimating Class Abundances from Chemical Marker – Application to HPLC Measurements of Phytoplankton Pigments. *CSIRO Marine Laboratories Report 229*, Hobart, Australia, pp.1-47.

Maiti, K., Charette, M., Buesseler, K. and Kahru, M. (2013). An inverse relationship between production and export efficiency in the Southern Ocean. *Geophysical Research Letters*, 40(8), pp.1557-1561.

Martiny, A., Pham, C., Primeau, F., Vrugt, J., Moore, J., Levin, S. and Lomas, M. (2013a). Strong latitudinal patterns in the elemental ratios of marine plankton and organic matter. *Nature Geoscience*, 6(4), pp.279-283.

Martiny, A., Vrugt, J. and Lomas, M. (2014). Concentrations and ratios of particulate organic carbon, nitrogen, and phosphorus in the global ocean. *Scientific Data*, 1, 140048.

Martiny, A., Vrugt, J., Primeau, F. and Lomas, M. (2013b). Regional variation in the particulate organic carbon to nitrogen ratio in the surface ocean. *Global Biogeochemical Cycles*, 27(3), pp.723-731.

McGlathery, K.J., Sundbäck, K., Anderson, I.C., 2004. The importance of primary producers for benthic nitrogen and phosphorus cycling. In: Nielsen, S.L., Banta, G.T., Pedersen, M.F. (Eds.), Estuarine Nutrient Cycling: The Influence of Primary Producers. *Aquatic Ecology Ser. 2*, pp. 231–261.

Meyer, J., Löscher, C., Neulinger, S., Reichel, A., Loginova, A., Borchard, C., Schmitz, R., Hauss, H., Kiko, R. and Riebesell, U. (2016). Changing nutrient stoichiometry affects phytoplankton production, DOP accumulation and dinitrogen fixation – a mesocosm experiment in the eastern tropical North Atlantic. *Biogeosciences*, 13(3), pp.781-794.

Morris, A. and Riley, J. (1963). The determination of nitrate in seawater. *Analytica Chimica Acta*, 29, pp.272-279.

Mullin, J. and Riley, J. (1955). The colorimetric determination of silicate with special reference to sea and natural waters. *Analytica Chimica Acta*, 12, pp.162-176.

Murphy, J. and Riley, J. (1962). A modified single solution method for the determination of phosphate in natural waters. *Analytica Chimica Acta*, 27, pp.31-36.

Nelson, D., Tréguer, P., Brzezinski, M., Leynaert, A. and Quéguiner, B. (1995). Production and dissolution of biogenic silica in the ocean: Revised global estimates, comparison with regional data and relationship to biogenic sedimentation. *Global Biogeochemical Cycles*, 9(3), pp.359-372.

Neuer, S. , Iversen, M. and Fischer, G. (2014). The Ocean's Biological Carbon Pump as Part of the Global Carbon Cycle. , *Limnology and Oceanography* e-Lectures, 4 (4), pp.1-51.

Paytan, A. and McLaughlin, K. (2007). The Oceanic Phosphorus Cycle. *Chemical Reviews*, 107(2), pp.563-576.

Quigg, A., Finkel, Z., Irwin, A., Rosenthal, Y., Ho, T., Reinfelder, J., Schofield, O., Morel, F. and Falkowski, P. (2003). The evolutionary inheritance of elemental stoichiometry in marine phytoplankton. *Nature*, 425(6955), pp.291-294.

Redfield, A. (1958). The biological control of chemical factors in the environment. *American Scientist*, 46(3), pp.230A, 205-221.

Riebesell, U., Czerny, J., von Bröckel, K., Boxhammer, T., Büdenbender, J., Deckelnick, M., Fischer, M., Hoffmann, D., Krug, S., Lentz, U., Ludwig, A., Muche, R. and Schulz, K. (2013).

Technical Note: A mobile sea-going mesocosm system – new opportunities for ocean change research. *Biogeosciences*, 10(3), pp.1835-1847.

Riebesell, U., Schulz, K., Bellerby, R., Botros, M., Fritsche, P., Meyerhöfer, M., Neill, C., Nondal, G., Oschlies, A., Wohlers, J. and Zöllner, E. (2007). Enhanced biological carbon consumption in a high CO2 ocean. *Nature*, 450(7169), pp.545-548.

Sharp, J. (1974). Improved analysis for "particulate" organic carbon and nitrogen from seawater. *Limnology and Oceanography*, 19(6), pp.984-989.

Shatova, O., Wing, S., Hoffmann, L., Wing, L. and Gault-Ringold, M. (2017). Phytoplankton community structure is influenced by seabird guano enrichment in the Southern Ocean. *Estuarine, Coastal and Shelf Science*, 191, pp.125-135.

Sommer, U., Hansen, T., Stibor, H. and Vadstein, O. (2004). Persistence of phytoplankton responses to different Si:N ratios under mesozooplankton grazing pressure: a mesocosm study with NE Atlantic plankton. *Marine Ecology Progress Series*, 278, pp.67-75.

Sterner, R., Andersen, T., Elser, J., Hessen, D., Hood, J., McCauley, E. and Urabe, J. (2008). Scale-dependent carbon:nitrogen:phosphorus seston stoichiometry in marine and freshwaters. *Limnology and Oceanography*, 53(3), pp.1169-1180.

Stoecker, D., Hansen, P., Caron, D. and Mitra, A. (2017). Mixotrophy in the Marine Plankton. *Annual Review of Marine Science*, 9(1), pp.311-335.

Turner, J. (2015). Zooplankton fecal pellets, marine snow, phytodetritus and the ocean's biological pump. *Progress in Oceanography*, 130, pp.205-248.

Wainright, S., Haney, J., Kerr, C., Golovkin, A. and Flint, M. (1998). Utilization of nitrogen derived from seabird guano by terrestrial and marine plants at St. Paul, Pribilof Islands, Bering Sea, Alaska. *Marine Biology*, 131(1), pp.63-71.

Welschmeyer, N. (1994). Fluorometric analysis of chlorophyll a in the presence of chlorophyll b and pheopigments. *Limnology and Oceanography*, 39(8), pp.1985-1992.

White, A. and Dyhrman, S. (2013). The marine phosphorus cycle. *Frontiers in Microbiology*, 4(105), pp.1-2.

Wootton, J. (1991). Direct and indirect effects of nutrients on intertidal community structure: variable consequences of seabird guano. *Journal of Experimental Marine Biology and Ecology*, 151(2), pp.139-153.

Yang, Y., Gao, B., Hao, H., Zhou, H. and Lu, J. (2017). Nitrogen and phosphorus in sediments in China: A national-scale assessment and review. *Science of The Total Environment*, 576, pp.840-849.

6. Appendix

Table 6.1: Concentrations of dissolved inorganic nitrogen species of the two OMZ derived water masses.

Water mass	NO_3^- (µmol L^{-1})	NO_2^- (µmol L^{-1})	NH_4^+ (µmol L^{-1})
Very low N:P	0.000	0.040	0.254
Low N:P	1.075	2.884	0.302

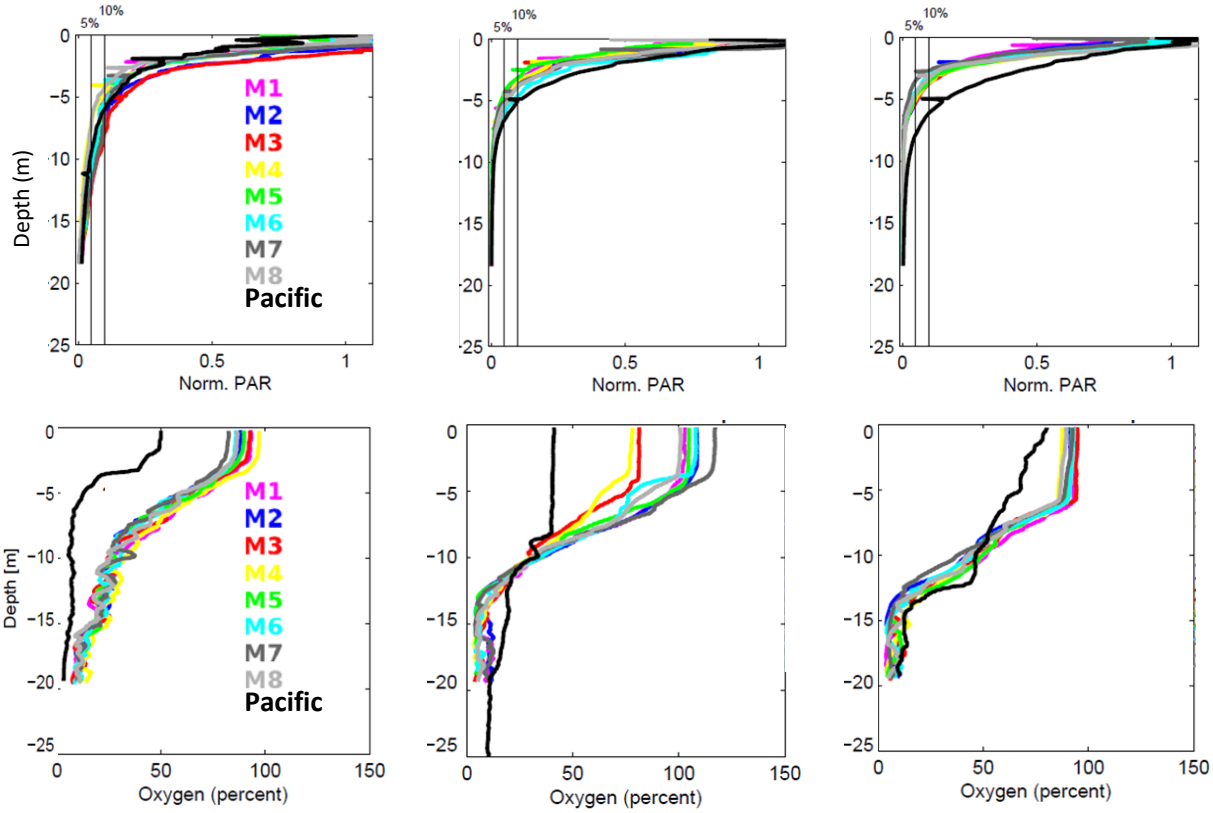

Figure 6.1: Photosynthetically active radiation levels (top) and oxygen content (bottom) in each of the mesocosms (M1-M8) and surrounding Pacific water for day 8 (left), 22 (middle) and 36 (right). Graphs provided by Kai Schulz.

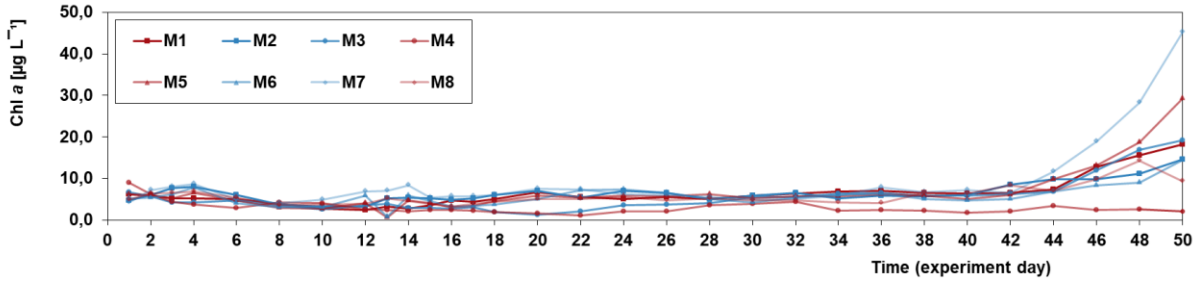

Figure 6.2: Depth integrated chlorophyll a concentrations in the water column for each mesocosm.

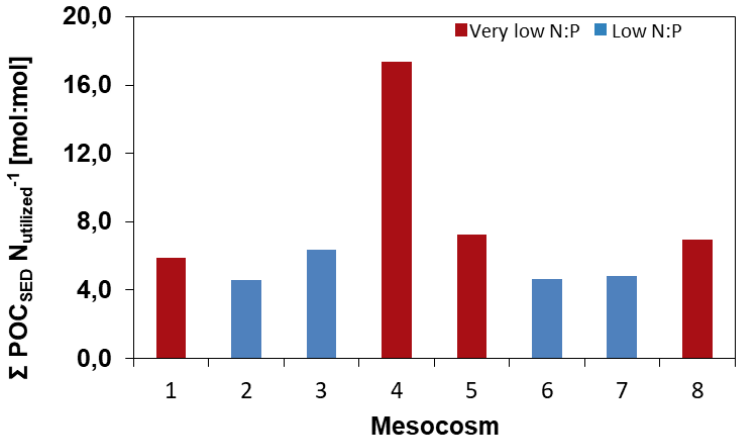

Figure 6.3: Carbon export to sediment traps per utilized N in the water column for each mesocosm

Table 6.2: Apparent total consumption of nitrogen (µmol L^{-1}) in each of the eight mesocosms over the entire experiment

	M1	M2	M3	M4	M5	M6	M7	M8
$N_{utilized}$	8.97	11.58	10.15	2.95	5.98	10.24	11.57	7.20

Table 6.3: Initial depth integrated chemical conditions in the eight mesocosms (all units in µmol L^{-1})

	M1	M2	M3	M4	M5	M6	M7	M8
NO_2^-	0.55	1.22	0.54	0.53	0.69	1.05	1.76	1.33
NO_3^-	6.29	5.82	6.36	5.07	5.81	5.92	5.83	5.55
NH_4^+	5.47	4.49	4.03	2.24	2.95	3.30	4.87	3.35
PO_4^{3-}	1.61	1.91	1.58	1.39	1.75	1.85	1.97	1.88
$Si(OH)_4^-$	7.96	10.01	7.43	6.12	8.82	9.52	10.35	9.63